TECHNICAL REPORT

Shear Tests on Glulam-CLT Joints with Double-Sided Punched Metal Plate Fasteners and Inclined Screws

Nicolas Jacquier

LULEÅ UNIVERSITY OF TECHNOLOGY

LULEÅ
UNIVERSITY
OF TECHNOLOGY

Shear Tests on Glulam-CLT Joints with Double-Sided Punched Metal Plate Fasteners and Inclined Screws

Nicolas Jacquier

Luleå University of Technology
Department of Civil, Environmental and Natural Resources Engineering
Division of Structural and Construction Engineering

Printed by Luleå University of Technology, Graphic Production 2014

ISSN 1402-1536
ISBN 978-91-7439-892-2 (print)
ISBN 978-91-7439-893-9 (pdf)

Luleå 2014

www.ltu.se

Table of Contents

Notations and symbols

A	anchorage area of the double-sided nail plates
b_{NP}	double-sided nail plate width
D_f	ductility ratio with respect to slip at failure (failure over yield slip)
D_u	ductility ratio with respect to slip at maximum load (slip at maximum load over yield slip)
D_{fu}	absolute ductility between slip at failure load and slip at maximum load [mm]
D_{fy}	absolute ductility between slip at failure load and yield slip [mm]
D_{uy}	absolute ductility between slip at maximum load and yield slip [mm]
d	screw diameter
F_{01}	$0.1 \times F_{est}$
F_{04}	$0.4 \times F_{est}$
F_{est}	Estimated maximum load in the test
F_{max}	maximum load measured in the test
F_{max}/A	maximum load per anchorage area of nail plate
F_{max}/n_s	maximum load per screw
k_i	initial slip modulus
k_s	slip modulus
L	screw length
l_{NP}	double-sided nail plate length
n_s	number of screws in the connection
t_i	double-sided nail plate teeth length
u_f	slip at failure load (chosen equal to $0.8 \times F_{max}$)
u_{max}	(= v_{max}) slip at maximum load F_{max}
$u_{y,EN}$	yield slip according to EN 12512 method
$u_{y,05Fmax}$	yield slip according to Karacabeyli and Ceccotti method
$u_{y,04\text{-}09}$	yield slip according to Yasumura and Kawai method
$u_{y,CSIRO}$	yield slip according to CSIRO Australia method
v_{01}... v_{24}	slip values at the measuring points according to EN 26891 loading procedure $f(F_{est})$
$v_{0,6}$	slip at $0.6 \times F_{max}$
$v_{0,8}$	slip at $0.8 \times F_{max}$
v_{max}	(= u_{max}) slip at maximum load F_{max}
$v_{i,mod}$	modified initial slip
v_s	joint settlement
v_e	elastic slip
$v_{i,mod}$ - v_{24}	slip to be added to v_{06} and v_{08} for their modified values
$\rho_{0,\omega}$	density of the timber with oven-dry weight and volume measured at testing moisture content ω
ρ_ω	density at moisture content ω
ω	moisture content

Subscripts:

c	CLT
g	Glulam
k	characteristic value
mean	mean value
0	either corresponds to the dry density or to a 0° angle

Abbreviations:

AG	Nail plate anchorage failure from the glulam
AC	Nail plate anchorage failure from the CLT
CoV	coefficient of variation
CLT	Cross Laminated Timber
DSNP	Double-sided nail plate
S1	S1_2S-6.5
S2	S2_2S-8.2
S3	S3_1NP-200/2S-6.5
S4	S4_1NP-200/2S-8.2
S5	S5_2NP-100/1S-6.5
S6	S6_2NP-100
S7	S7_1NP-100/2S-6.5
S8	S8_1NP-200
SA	SA_1NP-200
PTC	pull-through failure of screw in CLT
WG	withdrawal failure of screw in glulam

Abstract

A new shear connection system was tested in order to be used in off-site manufactured cassette floor elements made with glulam beams and Cross Laminated Timber (CLT) panels. The shear connection proposed is made with double-sided punched metal plate fasteners, connecting CLT and glulam members to form a T-cross-section. Due to the lack of withdrawal capacity of punched metal plate fasteners, the shear connection must be secured with screws to resist separations forces which may occur between the members in the floor element.

Shear tests were performed on glulam-CLT joints made with double-sided punched metal plate fasteners and with inclined self-tapping screws as reference cases to compare to joints with both fastener types combined. Each fastener type is characterised by a specific load-slip curve and different values for the yield slip, slip at maximum load and failure slip. These parameters can be used to evaluate the compatibility of the different fasteners and their combined effect in a joint. The test results show that there is a significant contribution from both the double-sided punched metal plate and inclined screw fasteners to the strength and stiffness of the combined joints.

Due to the fact that the individual fasteners reach their maximum load for different slip values, the load-carrying capacity of joints with combined fasteners is somewhat lower than the sum of the individual fasteners load-carrying capacities. The slip modulus of the combined fasteners may be estimated as the sum of the respective slip modulus of each fastener due to the compatible behaviour of the fasteners in the serviceability limit state.

1. Introduction

Timber floor elements for multi-storey buildings often need to reach long spans. The use of standard Cross Laminated Timber (CLT) panels for these applications leads to relatively thick CLT floor structures. In addition, these floor elements are often used as one way spanning structures, which is not the most advantageous configuration when using CLT due to the limited contribution of the cross layers. The combination of CLT panels with other engineered wood products can be beneficial in order to improve the bending stiffness and reduce the self-weight of CLT-based floor elements. This study focuses on the combination of horizontal CLT panels with glulam beams in order to form a prefabricated composite cassette floor unit.

There are several alternative ways to structurally connect glulam beams and CLT panels. One possibility is to connect them with the minimal effort and therefore not aiming for any composite action. This can be made by using the minimum amount of screws needed for the assembly and lifting purpose for example. This solution, which is not fully relevant from a structural performance point of view, can be beneficial with respect to other non-structural design aspects. In that situation the CLT panel can for example contribute to the fire protection, bracing to some extent, serve as an assembly support for floor element prefabrication, improve the sound absorption and or be used for aesthetic purpose if the CLT panels are left visible.

The second alternative is to structurally connect the glulam beams to the CLT panels with a certain amount of mechanical fasteners in order to reach a defined level of composite action. This can be done with self-tapping screws which can be oriented perpendicular or inclined with respect to the shear plane or p. The advantage of this solution is that it gives the possibility to be realised on-site or off-site. However, screw connectors, even inclined are limited in terms of capacity and stiffness and the labour cost for their installation is relatively high.

The third option is to use structural glue to connect glulam beams and CLT panels and therefore obtain a full composite action between members. However the gluing process is often demanding in terms of manufacturing facilities and quality controls (equipment for planning and pressing, controlled climate, curing time…). Press gluing and screw gluing processes are possible.

In this study the use of a new type of mechanical shear connector for glulam-CLT floor elements is investigated. Double-sided punched metal plate fasteners also called double-sided nail plates (DSNP) have been recently developed and represent an alternative solution for shear load transfer between timber members. Pressed between two timber members, they can provide high stiffness and load bearing capacity. The potential benefit of this type of connector is to provide with the possibility of rapid installation in off-site production of floor elements.

Preliminary shear tests were carried out at VTT in April 2012 in order to assess the behaviour of double-sided nail plate fasteners for glulam-CLT joints. The nail plate connection did perform well in shear in terms of load-carrying capacity and stiffness. However the post peak behaviour seemed uncertain. Very soon after the ultimate load the back-out of the nail plate occurs and the connected member fall apart as it is common for punched metal plate fasteners. This is partly due to the fact that double-sided punched metal plate fasteners have theoretically no withdrawal capacity which means that there is a risk for back-out of the nail plate if a separation force is introduced between the CLT

and glulam members. This separation force might be generated by dead loads, hanging loads, or by the effect of loaded members in bending with different bending stiffness. The connection therefore needs to be secured against separation forces.

In this phase of the study it was proposed to use screws in order to secure the shear connection made with double-sided nail plates. While the double-sided nail plates can provide most of the joint stiffness it is not economical to add a large amount of screws. The aim was therefore to add the minimum amount of screws. The screws used in this study are self-tapping screws inclined at 45° angle. Inclined screws were chosen due to the relatively high strength and stiffness that they can provide in this configuration and in order to benefit from the compressive force generated between the timber members when an inclined screws is loaded in shear tension.

Regarding the design of such joint with different types of fasteners combined, either the fasteners are considered to act independently with the double-sided nail plates resisting the shear forces and the screws the possible separation forces, either their simultaneous action can be considered, essentially with respect to the shear forces. If the combined action is considered with respect to the shear forces, the combination of mechanical fasteners of different nature in a joint needs to be evaluated both in terms of stiffness and in terms of load-carrying capacity.

One of the aims of this study is to evaluate if double-sided nail plates represent a suitable alternative to screwed or glued connection for the assembly of composite timber members. This study aims also at evaluating the combination of different types of mechanical fasteners in a joint.

This report is the first part of a test program performed at VTT (Finland) where shear tests and bending tests were carried out on composite members made from CLT panels and glulam beams.

2. Methods

The experimental program presented in this report was carried out at VTT Expert Services Laboratories in Finland in 2013.

Tests were carried out following the standard EN 1075:1999 “Timber structures - Test methods - Joints made with punched metal plate fasteners” [1]. The loading procedure given in EN 26891 [2] was followed except for the series S1, S6, and SA where the tests were run under load control until failure.

2.1. Materials

Sepa Oy delivered the double-sided nail plates Sepa-SE2P and SFS Intec AB the SFS-WT screws for the shear tests.

2.1.1. Double-sided nail plates

The double-sided nail plates Sepa-SE2P, according to the VTT’s statement VTT-S-02797-12 [3], had dimensions 72×100 and 72×200 (in mm), see Fig. 1.

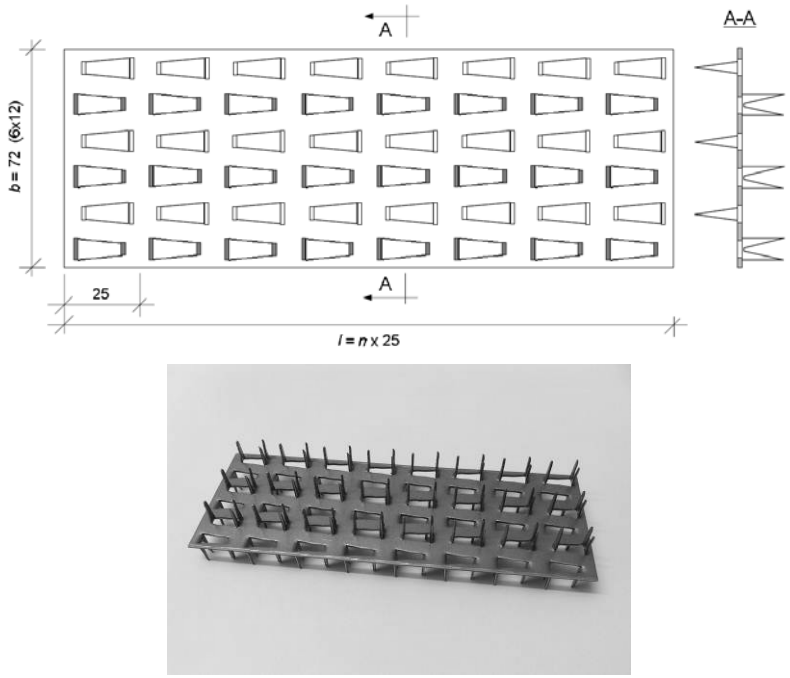

Fig. 1: Structure and dimensions of Sepa-SE2P nail plate 72×200, in mm. Teeth dimensions and spacing are according to SE35 nail plate (Statement VTT-S-08544-10).

The nail plates were delivered together with a manufacture’s inspection certificate of the steel plate material. Mechanical properties according to the manufacture’s inspection certificate were: tensile yield strength 410 N/mm^2, ultimate tensile strength 485 N/mm^2, elongation 28.0 % and weight of zinc coating 293 g/m^2.

2.1.2. Screws

SFS Intec screws WT were according to European Technical Approval ETA-12/0063 [4] with dimensions ($d \times L$ in mm) 6.5×160 and 8.2×160, see Fig. 2. Some of the mechanical characteristics according to the ETA-12/0063 [4] are reported in Table 1.

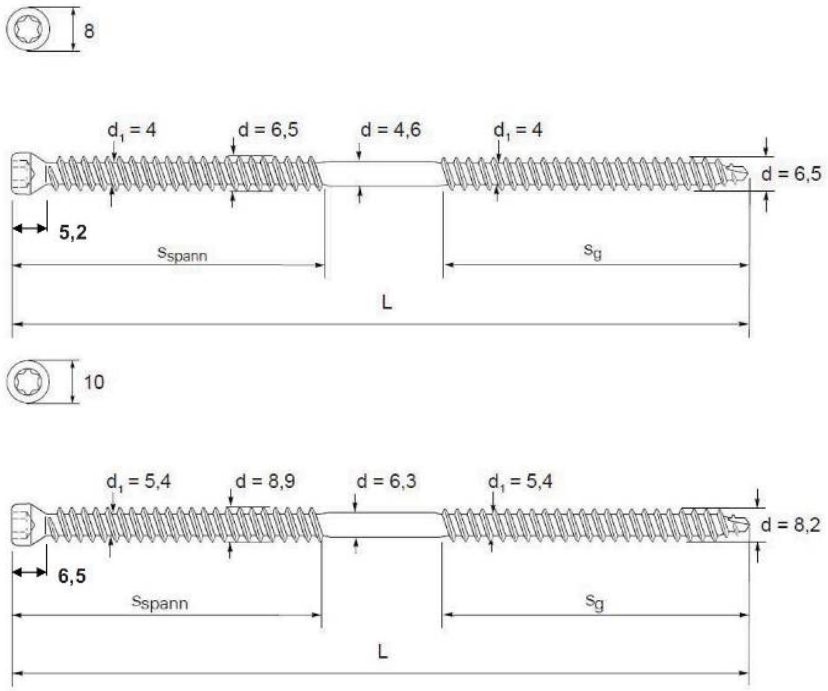

WT-T-6,5 × *L*

WT-T-8,2 × *L*

Fig. 2: Geometry and dimensions of SFS Intec WT self-tapping screws (source: ETA-12/0063 [4])

Table 1: Mechanical characteristics of SFS WT self-tapping screws according to ETA-12/0063 [4]

			WT-T-6,5 × *L*	WT-T-8,2 × *L*
Characteristic yield moment	$M_{y,k}$	[Nm]	12.7	19.5
Characteristic withdrawal parameter (angle screw-axis to grain 90°, ρ_k = 350 kg/m^3)	$F_{ax,k,90°}$	[N/mm^2]	12.9	13.35
Characteristics tensile capacity	$f_{tens,k}$	[kN]	14.4	28.6
Characteristic yield strength	$f_{y,k}$	[N/mm^2]	990	870

2.1.3. Timber

The glue laminated timber members were made out of Norway spruce (Picea abies) and labelled L40 (Nordic glulam strength class) corresponding to GL32 (SS-EN 1194 [5]). Cross Laminated Timber "*CLT Stora Enso*" according to European technical approval ETA-08/0271 [6] was used. CLT had been manufactured from solid wood lamellas of strength class C24 by Stora Enso Wood Products GmbH in Austria. The nominal characteristics for sawn timber C24 and glulam GL32 and are reported in Table 2 for information.

Table 2: Mechanical properties for solid wood C24 and for glulam GL32
(Characteristic strength and stiffness values in N/mm^2 and densities in kg/m^3 for selected strength classes of softwood and softwood glulam)

Property		**Strength classes**	
		C24	**GL32**
Bending strength	$f_{m,k}$	24	32
Tension strength	$f_{t,0,k}$	14	22.5
Tension perp. to grain	$f_{t,90,k}$	0.4	0.50
Compression strength	$f_{c,0,k}$	21	29
Compression strength perp.to grain	$f_{c,90,k}$	2.5	3.3
Shear strength	$f_{v,k}$	4.0	3.8
Mean modulus of elasticity	$E_{0,mean}$	11000	13700
Lower 5-percentile modulus of elasticity	$E_{0,05}$	7400	11100
Mean modulus of elasticity perp. to grain	$E_{90,mean}$	370	460
Shear modulus	G_{mean}	690	850
Characteristic density	ρ_k	350	430
Mean density	ρ_{mean}	420	520

The glulam and CLT material were selected in accordance with method 2 in EN 28970 [7] with a targeted characteristic density of glulam $\rho_{g,\omega,k}$ = 380 kg/m^3 and $\rho_{c,\omega,k}$ = 350 kg/m^3 for CLT in an environment with relative humidity of 65% and temperature 20°C. The glulam members of cross section of 90×150 mm^2 were split from the beam size 90×315 mm^2 by VTT. The lamella thickness of glulam was 45 mm. The dimensions of the delivered CLT panels were 60×250×2500 mm^3. CTL was composed of three 20 mm thick layers.

2.2. Test specimens

The timber materials were first stored in climate room with RH 85 % and T 20 °C for 5 weeks. After the nail plates were assembled the test specimens and the timber members of the screwed test specimens were stored for about three weeks in climate room with RH 65 % and T 20 ºC before the loading tests. Moisture content ω during the tests and densities ρ_ω and $\rho_{0,\omega}$ of the outer lamellas under the joint line were determined immediately after loading tests for each test specimens. The measured moisture contents and densities are presented in Table 4 in the results section.

For each test specimen, a 600 mm length of glue laminated timber member was cut so that the lamella of the connection side came from the different original lamella for each test specimens of the test series. CLT members were sawn with the same principle to the length of 600 mm. The outer lamellas of CLT were parallel to the length of the member. The nail plates and screws were assembled to the middle line of timber members (see Fig. 4). The connection was always on the outer lamella side of

the original glulam beam (90×315 mm^2). The configuration of the specimens, fasteners location and details for each test series are given in Fig. 4, Fig. 5 and
Table 3. The test series SA_1NP-200 was not part of the main test program presented in this report. These results are taken from VTT research report VTT-S-02784-12 [8] on tests performed in April 2012 on CLT-Glulam shear connections with the same 72×200 mm double-sided nail plates, and where this series was noted SE2P-A. They are included in this report since test series S8 and SA are comparable test series. The only differences between them are the glulam strength class used and the length of the test specimens which were respectively GL28c, and 500 mm in SA-1NP-200 and GL32 and 600 mm in the test series S8_1NP-200.

For the fabrication of the test specimens the double-sided nail plates were first compressed to the CLT members using a steel comb ribbed for nail plate teeth of compression side. Then the glulam members were pressed onto the nail plates. The double-sided nail plates were fastened by MTS testing machine by a deformation guided compression (5 mm/s) with a maximum load limitation of 55 kN so that the nail plates came to full contact with both timber members. The screws of the test specimens were assembled just before testing. The screwing angle was 45° for all tests (see Fig. 5). The screws were tightened so that no gap was left between timber members. However, in the specimens with nail plates, the exiting gap of 1 to 2 mm due to the double-sided nail plate thickness was not closed by the application of the screws.

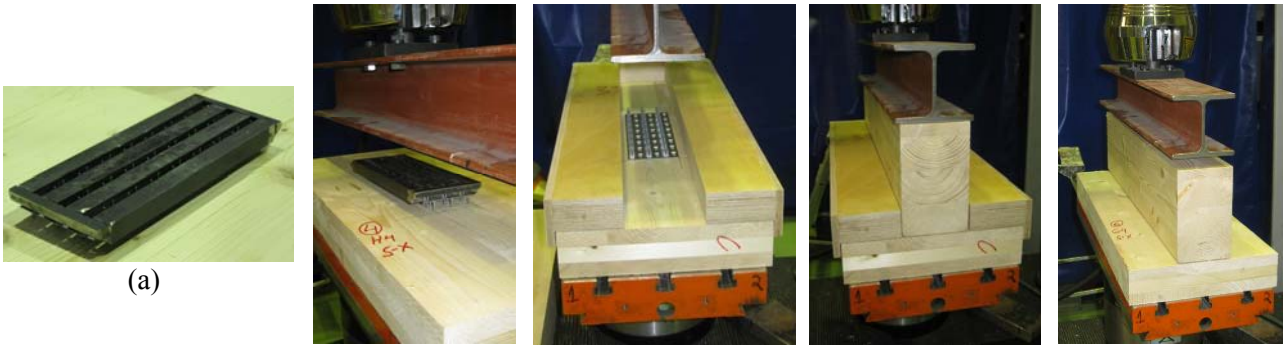

Fig. 3: Fabrication process for the test specimens with double-sided punched metal plate

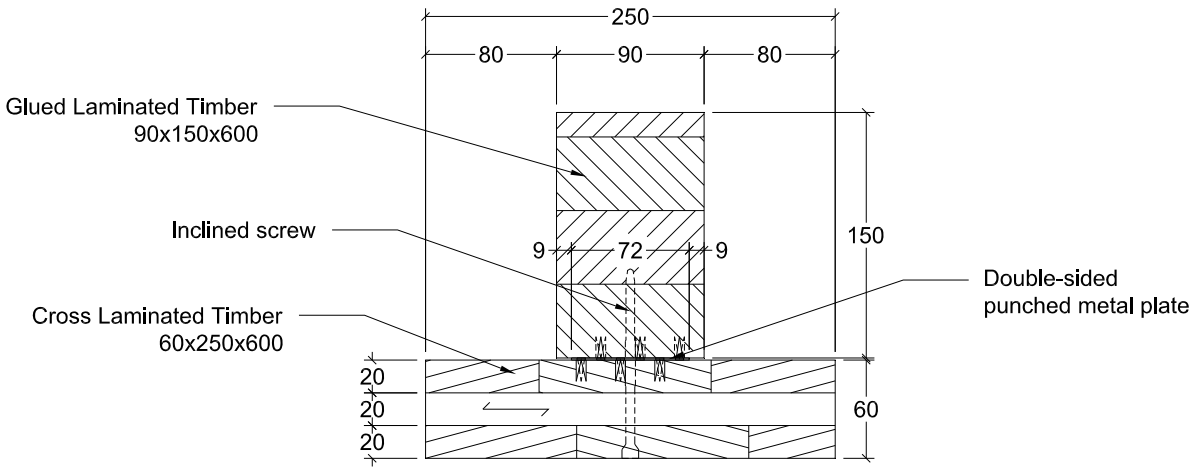

Fig. 4: Cross section of the shear test specimen.

Table 3: Test series for shear tests of glulam-CLT connections

Test series		Specimens		Screws		Double-sided nail plates (DSNP)		
Name	Name in VTT Report [8], [9]	No. of tests	F_{est}	No. of Screws	$d \times L$	No. of DSNP	$b_{NP} \times l_{NP}$	Total DSNP area
			kN		mm		mm	mm^2
S1_2S-6.5	S-1-6.5	4[1]	15	2	6.5 × 160	-	-	-
S2_2S-8.2	S-1-8.2	4[1]	20	2	8.2 × 160	-	-	-
S3_1NP-200/2S-6.5	S-3-6.5	6	50	2	6.5 × 160	1	72 × 200	14400
S4_1NP-200/2S-8.2	S-3-8.2	6	55, 50	2	8.2 × 160	1	72 × 200	14400
S5_2NP-100/1S-6.5	S-2	6	40	1	6.5 × 160	2	72 × 100	14400
S6_2NP-100	S-0	6	35	-	-	2	72 × 100	14400
S7_1NP-100/2S-6.5	S-4	6	30	2	6.5 × 160	1	72 × 100	7200
S8_1NP-200	S-8	6	35	-	-	1	72 × 200	14400
SA_1NP-200	SE2P-A	5	30	-	-	1	72 × 200	14400

d and L are the screw outer thread diameter and screw length, b_{NP} and l_{NP} are the double-sided nail-plate width and length, respectively. F_{est} is the estimated maximum load used in the loading procedure [2].

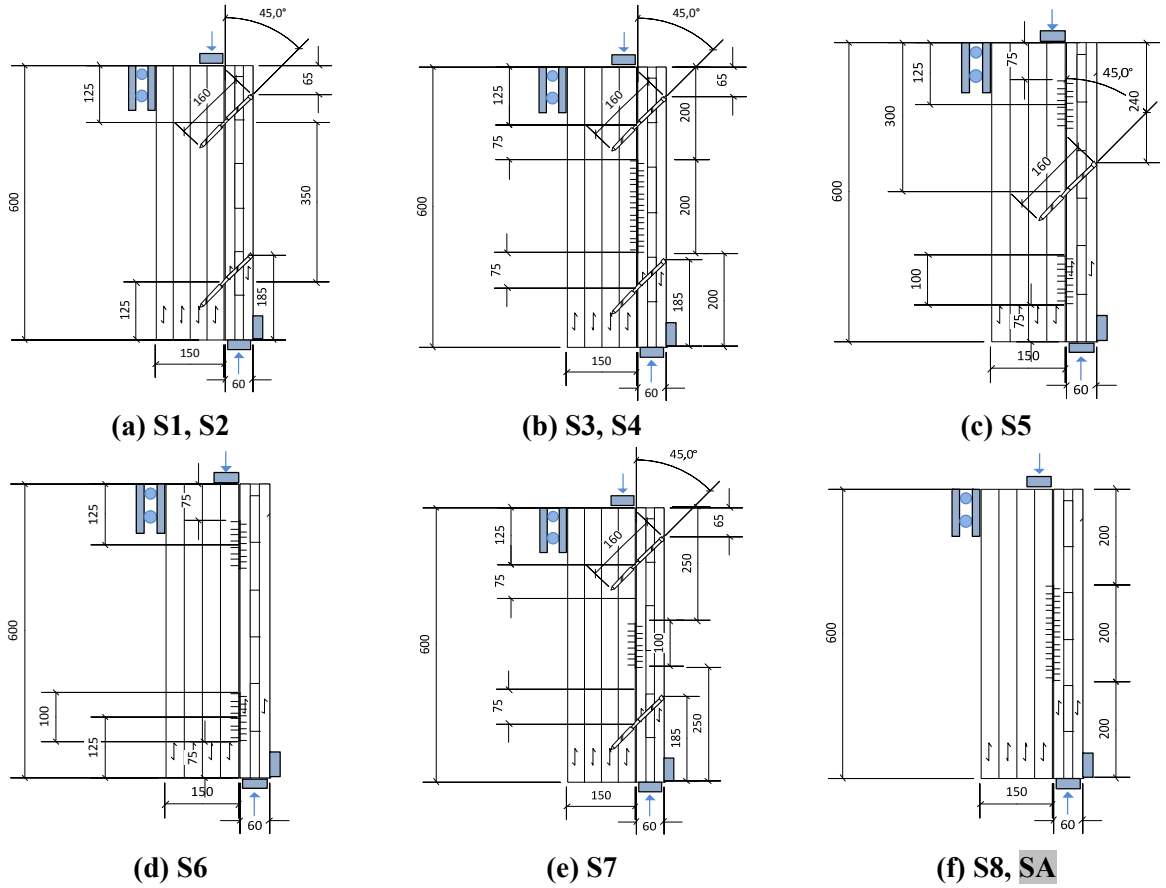

Fig. 5: Test setup for the shear test series S1 to S8

[1] Six tests were planned and performed but due to errors in manufacturing some of the test specimens, a slight gap was created between the members. Due to the influence of the gap on the test results, only four tests for which manufacturing was correct are considered for this test series. The load-slip curves of the full test series including the discarded test results are presented in Appendix A

2.3. Test setup

Test specimens were loaded by MTS materials testing machine with the calibrated compression capacity of 250 kN. The deformation measuring device was HBM displacement transducers W10 (± 10 mm). The loading procedure according to EN 26891 [2] was followed, where the loading rate was $0.2\times F_{est}$/min, with F_{est} the estimated load (cf. Table 3), up to $0.7\times F_{est}$ when a constant rate of slip was used (deformation controlled) up to failure. However, by mistakes the change to deformation control was not done for series S1 and S6 where the tests were run under load control until failure. Tests were intentionally stopped after 15 mm slip. Specific slip measurements points as given in EN 26891 [2] (cf. Fig. 7) are reported in Appendix B for each test specimen.

The loading arrangements were according the guidelines given in EN 1075 [1] for testing of fastener shear capacity. A general view of the loading arrangements is shown in Fig. 6. The angle θ between the gap line and the line drawn through the load point and centre point of the connection was 8°.

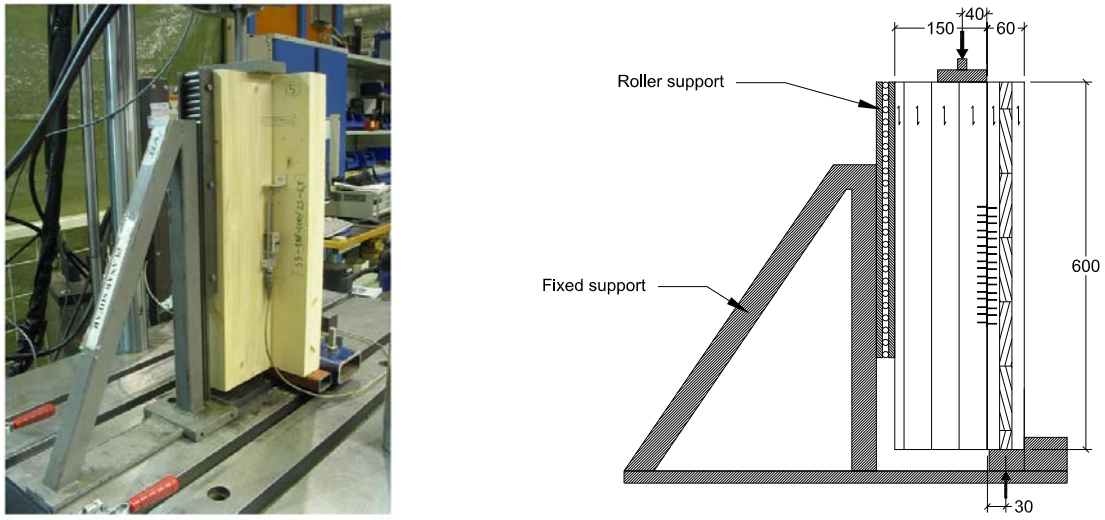

(a) (b)

Fig. 6: Shear tests setup (dimensions in mm)

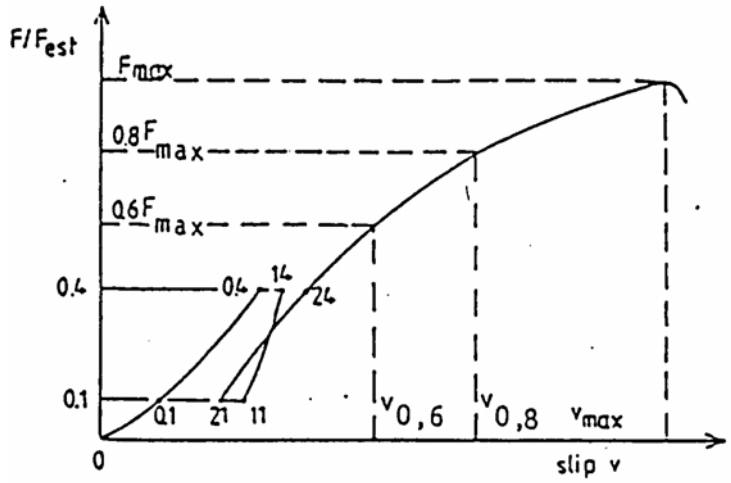

Fig. 7: Measuring points of load-slip curves according to EN 26891 for the evaluation of the slip modulus

2.4. Evaluation methods of the ductility and compatibility of the shear connectors

In order to compare the behaviour of the different mechanical fasteners used in this test program and assess the compatibility of their load-slip curves for a combined use, existing methods for evaluating the ductility of timber joints were used.

2.4.1. Yield slip

The yield slip, noted u_y, defines the limit of the linear response of the fastener on the load-slip curve. This parameter can be necessary for the evaluation of the joint ductility depending on the method adopted. There is today no consensus within the scientific community to prescribe a single method to determine the yield slip [10], [11] and the methods available lead to different results. In this report, each test series is evaluated according to four of the methods presented in [10] and the nomenclature for the yield slip according to these different methods in is as follows and is illustrated in Fig. 8 (for a more detailed explanation of the methods, refer to [11]):

- $u_{y,EN}$ for the EN 12512 method [12]
- $u_{y,05Fmax}$ for the method by Karacabeyli and Ceccotti referred in [10].
- $u_{y,04-09}$ for the method by Yasumura and Kawai referred in [10].
- $u_{y,CSIRO}$ for the method from CSIRO Australia [10], [11].

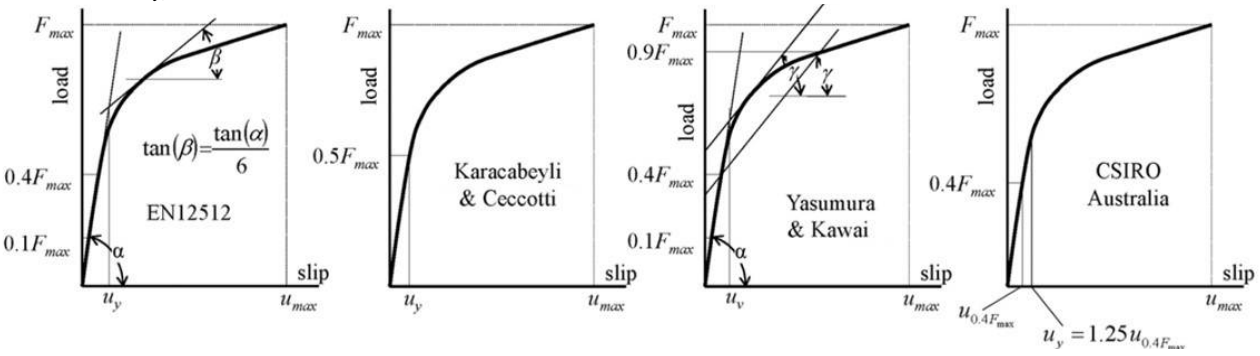

(a) (b) (c) (d)

Fig. 8: Methods for estimating the yield slip (after [10] and [11]), (a) $u_{y,EN}$, (b) $u_{y,05Fmax}$, (c) $u_{y,04-09}$, (d) $u_{y,CSIRO}$

2.4.2. Joint ductility

As mentioned, several methods exist for the evaluation of the ductility and an overview of them was presented in [13]. In this report, five of these definitions are considered. Two are expressions (1) and (2) which are given in EN 12512 [12], and are relative definitions [10]. Other definitions (3), (4), and (5) were proposed by Stehn and Björnfot [13] and are absolute definitions. In these expressions, u_y is the yield slip, u_{max} is the slip at maximum load, and u_f is the failure slip considered as the slip observed on the descending part of the load-slip curve after the maximum load when the load has decreased down to $0.8 \times F_{max}$. These definitions can be used as a mean of comparison between the test series. The joint ductility estimated according to each of these methods is presented in Appendix B considering the yield slip u_y from the EN 12512 [12] method only ($u_y = u_{y,EN}$). In Table 5, the mean value for each test series is presented.

$$D_f = \frac{u_f}{u_y} \quad (1) \qquad D_u = \frac{u_{max}}{u_y} \quad (2)$$

$$D_{uy} = u_{max} - u_y \quad (3) \qquad D_{fy} = u_f - u_y \quad (4)$$

$$D_{fu} = u_f - u_{max} \quad (5)$$

3. Results

3.1. Overview

The load-slip curves for each test series are presented in sections 3.2 to 3.4. Tables with detailed results for all shear tests series are presented in Appendix B.

An overview of the all test results is presented in Fig. 9 with a plot of the mean load-slip curve for each test series. The mean load-slip curve for each series were obtained by removing the unloading cycle between $0.1 \times F_{est}$ and $0.4 \times F_{est}$ of each load-slip curve and by averaging the load observed at a defined slip interval (0.02mm). The mean load-slip curve is truncated at 15 mm slip or at the lowest maximum slip value recorded for any test specimen in the test series. For series S1 and S6, the curves are represented with a dashed line from the instant when the loading protocol differed from the 26891 [2] as described in section 2.3, i.e. load control instead of deformation control. For the series S7, one curve of the series was removed when creating the mean load-slip curve due to a strange post-peak behaviour but the data up to the maximum load is considered in the test results for this series (all curves for series S7 are presented in Appendix A)

The mean load-slip curves are used as a simplified presentation of the test series and for summation of different test series in order to verify the superposition principle between them where it could be applicable.

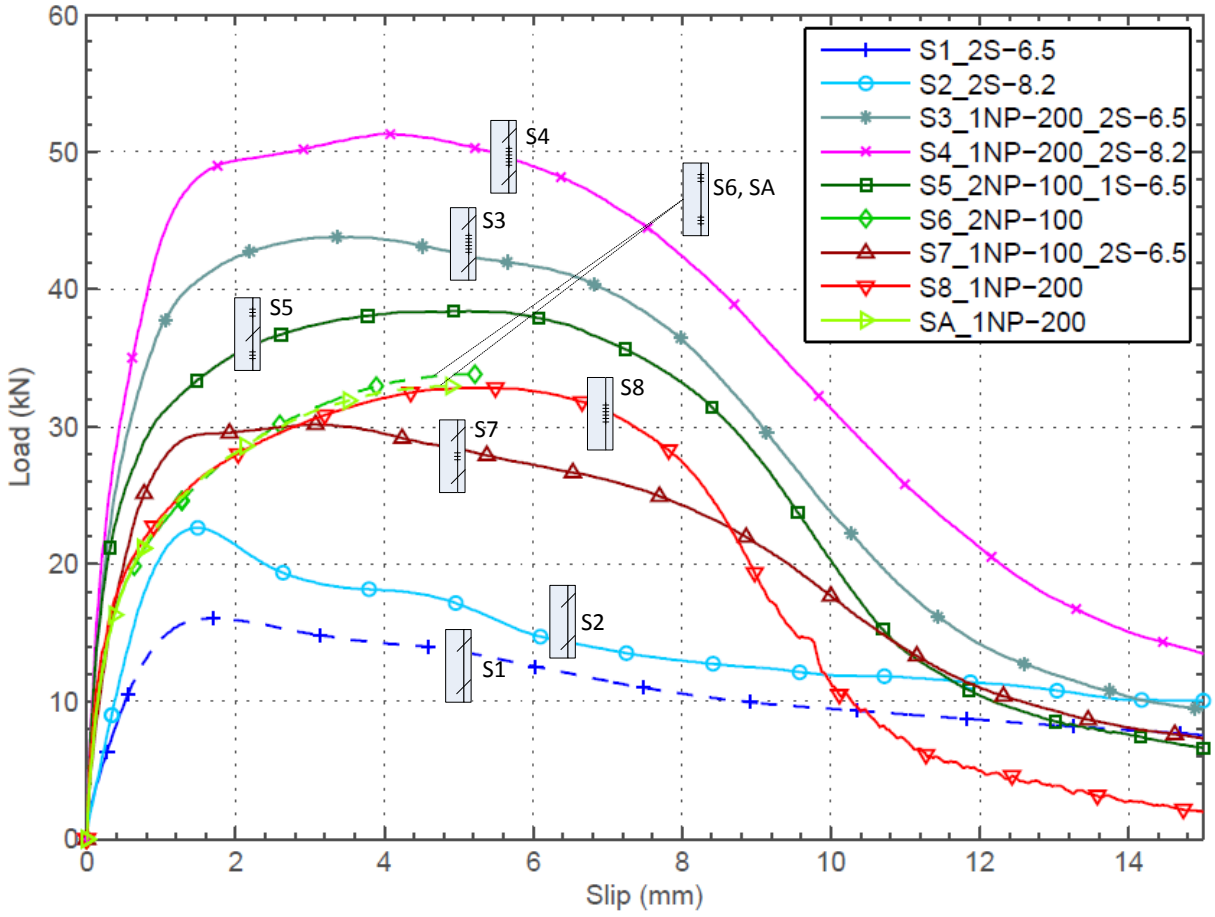

Fig. 9: Overview of the shear test results (mean load-slip curve for each test series)

The mean values for the ultimate load, slip at ultimate load and slip modulus for each test series are presented in Table 4. These values are calculated based on the individual load-slip curves. All test results are presented with six specimens per test series, except for the series S1_2S-6.5 and S2_2S-8.2, where only four tests results are considered due to some errors in the manufacturing process of the test specimens, and SA_1NP-200 where 5 tests were considered. The load-slip curves including the discarded tests are presented in Appendix A for the series S1, S2 and S7. Detailed results are including the specific slip measurements are presented in Appendix B.

The average densities measured of both the glulam and the CLT are similar despite of their different timber grades. The average density measured for all test series for the glulam is 458 kg/m^3. This value is well below the expected mean density for the strength class GL32, which should be about 520 kg/m^3. The average density measured for the CLT is 456 kg/m^3. This value can be compared with the mean value for glulam GL24h which should be about 440 kg/m^3. This value is common for CLT [14].

The failure of the fasteners was rather balanced between the CLT and the glulam. In each test series, it was possible to observe that the failure could occur either in the CLT, either in the glulam member, or sometimes in both members within the same test specimen when there were several fasteners in the joint. The failure had however a tendency to occur more often in the glulam member, both for the double-sided nail plate and the screw fasteners. Concerning the double-sided nail plates, this might be related to the fact the nail plates are pressed first into the CLT member. For the screws, there might be an effect due to the fact the head of the screw is in the CLT member which might improve the pull-through resistance in the CLT.

In Fig. 9, the different nature of the mechanical fasteners used can be observed in the tests series made with one type of fastener only (series S1, S2, S6, S8, SA). The joints with inclined screws only (series S1 and S2) exhibit a relatively long elastic regime with respect to their ultimate capacity and a low slip at failure. The post-peak behaviour is characterised by a rather gradual diminution of the load-carrying capacity until the end of the test (15 mm of slip). The joints with double-sided nail plates only (S6, S8, SA) are characterised by a more plastic behaviour before ultimate load. The slip at failure is high compared with the joint with inclined screws. The post-peak behaviour is characterised by a rapid decrease of the load bearing capacity. Test series where inclined screws and double-sided nail plates are combined exhibit a behaviour which is in-between the ones of the individual fasteners.

Table 4: Shear test results, mean values for the test series and failure observations

Test series	Notation in VTT reports [8], [9]	No. of tests	Glulam		CLT		Maximum load	Slip at maximum load	Slip modulus	Failure observations after the tests			
			$\rho_{g,\omega}$ kg/m^3	ω_g %	$\rho_{c,\omega}$ kg/m^3	ω_c %	F_{max} (CoV) kN (%)	u_{max} (CoV) mm (%)	k_s (CoV) kN/mm (%)	DSNP		Screws	
										AG	AC	WG	PTC
S1_2S-6.5	S-1-6.5	4	456	12.2	471	12.4	16.1 (5.3)	1.78 (9.4)	19.4 (7.3)	-	-	7	1
S2_2S-8.2	S-1-8.2	4	462	12.4	459	12.3	22.8 (10.6)	1.54 (11.0)	25.4 (9.3)	-	-	7	1
S3_1NP-200/2S-6.5	S-3-6.5	6	467	12.6	457	12.9	44.1 (6.2)	3.48 (17.5)	72.2 (12.4)	4	2	5	7
S4_1NP-200/2S-8.2	S-3-8.2	6	451	12.5	460	12.8	51.5 (7.2)	4.18 (11.3)	85.0 (10.4)	4	2	8	4
S5_2NP-100/1S-6.5	S-2	6	461	12.5	451	13.1	38.5 (3.5)	4.84 (11.2)	80.8 (7.8)	11	1	3	3
S6_2NP-100	S-0	6	444	12.7	450	13.8	33.9 (4.9)	5.20 (7.1)	45.8 (21.0)	7	5	-	-
S7_1NP-100/2S-6.5	S-4	6	452	12.4	457	12.8	30.1 (2.2)	2.85 (17.0)	46.9 (7.7)	4	2	7	5
S8_1NP-200	S-8	6	473	13.0	446	13.7	32.9 (2.9)	5.26 (8.8)	53.6 (7.8)	3	3	-	-
SA-1NP-200*	SE2P-A	5	451	12.7	406	11.8	33.2 (6.3)	5.27 (12.7)	12.7	3	2	-	-

* This test series is added here for comparison with test series S8. Tests were performed in April 2012 on a similar test setup [8]. Notable differences were: a specimen length of 500 mm instead of 600 mm and glulam GL28c was used instead of GL32.

The subscripts *c* and *g* denote the CLT and glulam members, respectively.

ρ_ω density at the moisture content at the time of testing calculated $\rho_\omega = \frac{m_\omega}{V_\omega}$ where m_ω is the wood sample mass at the time of testing and V_ω is the volume of the wood sample at the time of testing.

ω moisture content at the time of testing in % calculated $MC = \frac{m_\omega - m_0}{m_0} \cdot 100$ where m_ω is the wood sample mass at the time of testing and m_0 is the sample mass after drying.

CoV coefficient of variation in % calculated $CoV = \frac{\sigma}{\bar{x}}$ where $\bar{x}$ is the sample mean and σ is the sample standard deviation, estimated by $\sigma = \sqrt{\frac{1}{(n-1)} \sum_{i=1}^{n} (x_i - \bar{x})^2}$ where $\bar{x}$ is the sample mean, x_i is the i^{th} individual test value of the sample and *n* is the sample size.

AG double-sided nail plate anchorage failure from the glulam member

AC double-sided nail plate anchorage failure from the CLT member

WG withdrawal failure of screw in the glulam member

PTC pull-through failure of screw in CLT member

The mean values for the yield slip according to the different evaluation methods (cf. section 2.4) and the different ductility parameters are presented in Table 5. These results are also reported in Fig. 10, and Fig. 12. In Fig. 11, the mean values for the yield slip according to EN 12512, the slip at maximum load and the failure slip are presented.

Table 5: Mean values of specific slip values and ductility evaluations

	Test series	S1*	S2	S3	S4	S5	S6*	S7	S8	SA*
$u_{v,EN}$	(EN 12512)	0.67	0.79	0.34	0.38	0.25	0.33	0.48	0.27	0.37
u_{max}		1.78	1.54	3.48	4.18	4.84	5.19	2.85	5.26	5.27
u_f		5.69	3.41	8.28	8.42	8.50	6.74	7.52	8.47	6.59
D_f	($u_f / u_{v,EN}$)	8.78	4.29	24.52	22.44	34.73	20.69	15.87	31.72	17.91
D_u	($u_{max} / u_{v,EN}$)	2.73	1.94	10.37	11.14	19.81	16.05	5.98	19.69	14.41
D_{uv}	($u_{max} - u_{v,EN}$)	1.11	0.74	3.15	3.80	4.60	4.86	2.37	4.99	4.90
D_{fv}	($u_f - u_{v,EN}$)	5.02	2.61	7.94	8.04	8.25	6.41	7.05	8.21	6.22
D_{fu}	($u_f - u_{max}$)	3.91	1.87	4.80	4.24	3.65	1.54	4.68	3.21	1.32
$u_{y,05Fmax}$	(Karacabeyli et al.)	0.38	0.44	0.30	0.33	0.26	0.41	0.31	0.33	0.40
$u_{y,04-09}$	(Yasumura et al.)	0.42	0.54	0.29	0.29	0.26	0.34	0.33	0.30	0.37
$u_{y,CSIRO}$	(CSIRO)	0.35	0.43	0.25	0.27	0.21	0.31	0.28	0.25	0.32

* Results including u_f for series S1, S6 and SA should be considered with care since the tests were fully run under load control and part of the curve after the maximum load might not be available or not be reliable.

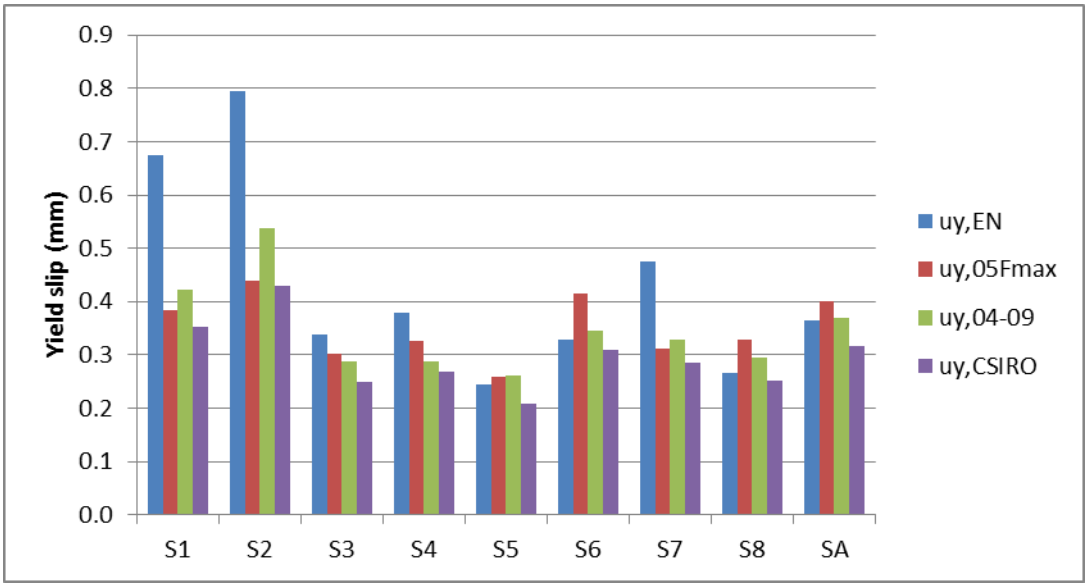

Fig. 10: Test series mean values for the yield slip according to the different methods

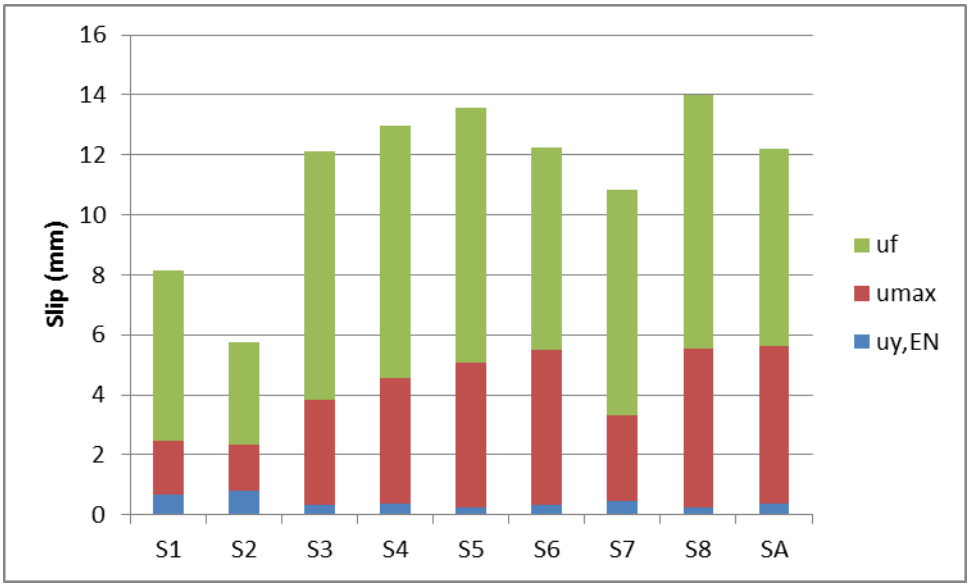

Fig. 11: Test series mean values for the yield slip (EN 12512), slip at maximum load and slip at failure load

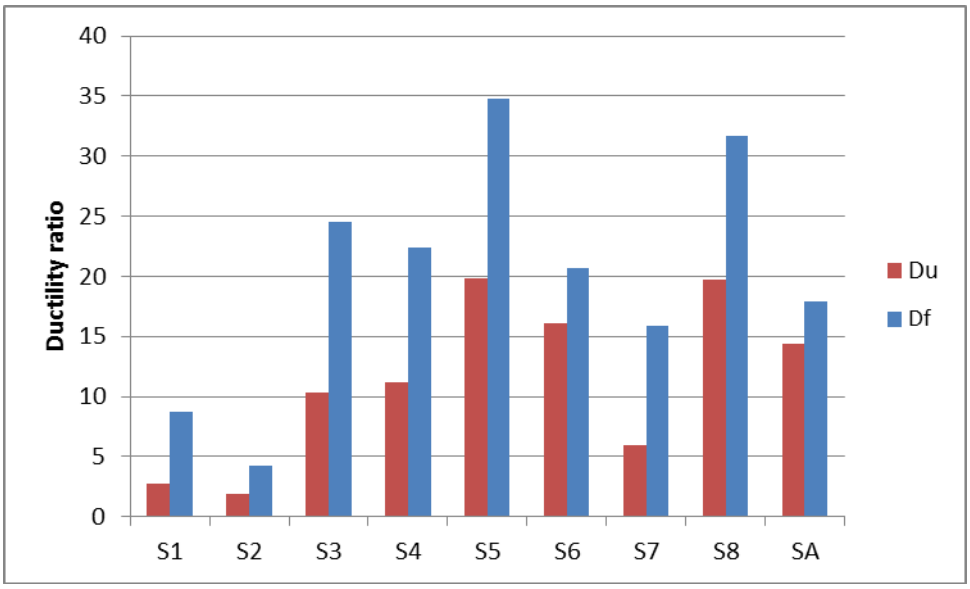

Fig. 12: Test series mean values for the ductility ratios according to EN 12512

3.2. Series with inclined screws only (S1, S2)

In test series S1 and S2, joints with two inclined screws at 45° were tested with different screws diameters, 6.5 and 8.2 mm respectively. Similar behaviours are observed for series S1 and S2, Fig. 13 and Fig. 14, respectively. The inclined screw shear connections showed a high stiffness and ultimate load capacity compared to a shear connection with screws at an angle of 90° with the shear plane as shown in [15] where shear tests with similar self-tapping screws were performed with varying angles between the screw and the grain direction.

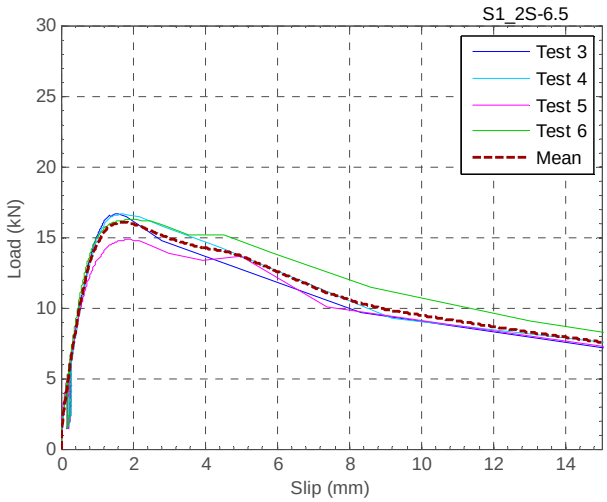

Fig. 13: Load-slip curves - S1_2S-6.5*

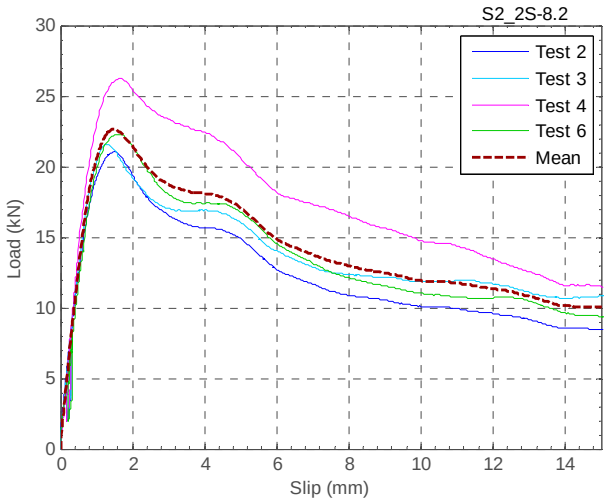

Fig. 14: Load-slip curves - S2_2S-8.2

*In Fig. 13, the curve is not very reliable after the peak load since the test series S1 was run under load control and therefore, the post peak loading was very rapid and only few data points are available.

Prior to the ultimate load, the withdrawal of the screw is governing the behaviour of the joint. With respect to the ultimate load, a long linear behaviour is visible. The joint stiffness (slip modulus k_s) increase observed from series S1 to series S2 is 31%, while the increase in screw diameter is 26%.

The failure is a withdrawal failure with either pull-out of the screw from the glulam member or a pull through of the screw in the CLT. Most of the time, the withdrawal of the screw occurs in one of the timber member and seldom in both members at the same time. Once the withdrawal or pull-through strength in one of the timber members is reached the capacity decreases gradually and the withdrawal failure propagates within this member. The joint is characterised by a low slip at maximum load u_{max}, 1.8 and 1.5 mm for screw diameters of 6.5 mm and 8.2 mm, respectively. The slip at failure (failure load considered as $0.8 \times F_{max}$) is in average 5.7 mm and 3.4 mm for screw diameters of 6.5 mm and 8.2 mm, respectively.

The remaining load-carrying capacity at 10 mm slip is above 50 % of the maximum load-carrying capacity. For large displacements, over (10 mm of slip) a gap tends to open at the top of the test specimen between the glulam and the CLT. The friction between the members can represent a significant part of the load-carrying capacity until the gap opens between members.

Due to the inclination of the screws, the dowel effect of the screw limited. However, it was possible to observe after the tests that small plastic hinges had formed, often in the head-side threaded part of the screw close to the middle of the screw. However, it is not possible to determine at which moment the hinges

developed. It is likely that they have formed after a significant displacement was applied after the maximum load was reached.

Fig. 15: Specimens of test series S2 after failure

Concerning the yield slip of the joints with inclined screws, the different methods for estimating the yield point give significantly different results (cf. Table 5). The EN 12512 [12] method is giving the highest results but can be appreciated as the most appropriate method to evaluate the inclined screws according to the observed shape of the load-slip curve, see Fig. 16. The observed yield slip is in this case relatively high with respect to the slip at maximum load. The ratio u_{max}/u_y is low which means that the plastic deformation after the yield point is limited before the maximum load is reached.

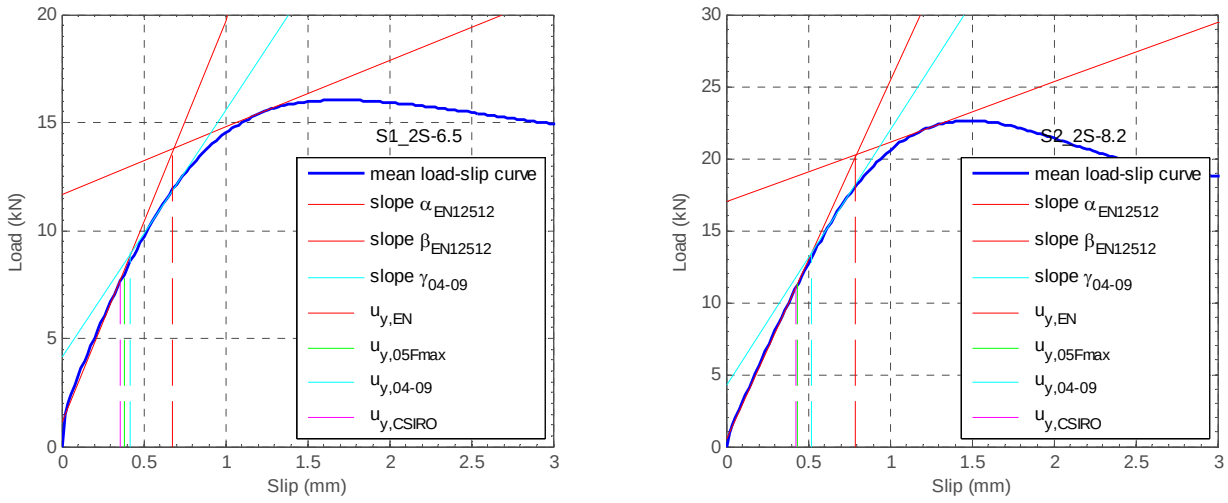

(a) (b)

Fig. 16: Evaluation of the yield slip on the mean load-slip curve, (a) S1, (b) S2

3.3. Test series with double-sided nail plates only (S6, S8, SA)

In test series S6, S8 and SA, joints with double-sided nail plates only were used. In series S6, a nail plate of length 200 mm was split in two pieces resulting in two double-sided nail plates of 100 mm length, while in series S8 and SA, one double-sided nail plate of length 200 mm was used. Similar behaviours are observed for series S6, S8 and SA on Fig. 17, and Fig. 19, respectively. The load-slip curves on Fig. 18 differ from the ones on the other two figures due to the loading which was displacement controlled after $0.7\times F_{est}$ in series S8 while it was entirely load controlled for series S6 and SA. For all series the loading procedure up to $0.7\times F_{est}$ was load controlled.

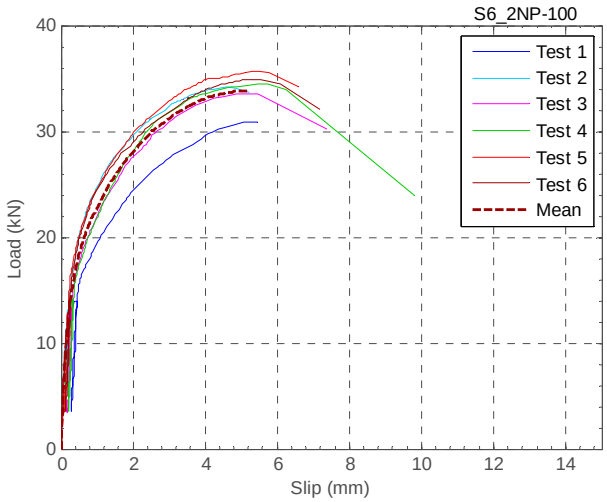

Fig. 17: Load-slip curves - S6_2NP-100

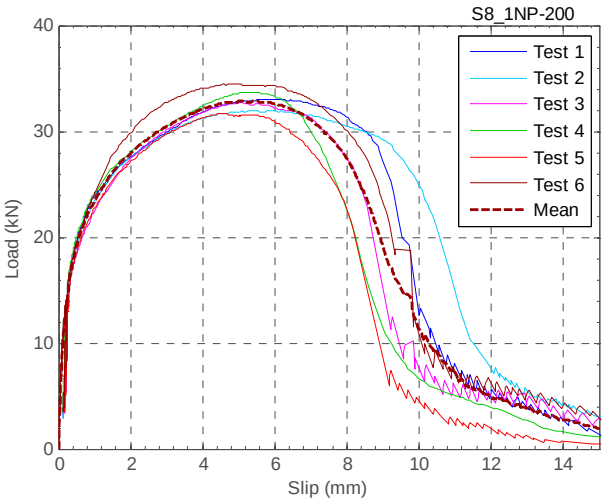

Fig. 18: Load-slip curves - S8_1NP-200

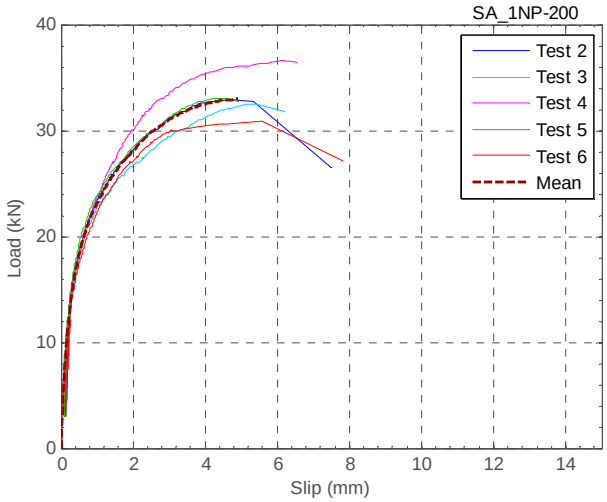

Fig. 19: Load-slip curves - SA_1NP-200

The double-sided nail plate joints present high load-carrying capacity and high initial stiffness. The connection starts to yield significantly after 50% of the maximum load. The mean value for slip at maximum load u_{max}, ranges from 5.2 to 5.3 mm for all series (cf. Table 5). The post-peak plastic deformation capacity and reserve strength capacity are very limited. At the end of the test, the glulam and CLT members are totally separated.

According to the load-slip curves, the double-sided nail plates shear connections behave in a similar way when the nail plate is in one piece or when it is divided in two pieces. Some difference in the results between these two configurations can be attributed to the position of the nail plates in the joint.

The failure is caused by the simultaneous bending of the teeth of the nail plates in both timber members and the crushing of the wood in front of the teeth. As the slip increases, the teeth bend and are withdrawn from their original position, contributing to open the gap between the timber members. The load-carrying capacity significantly decreases when the gap opens and while the double-sided nail plate is withdrawn from one of the timber member. The withdrawal of the double-sided nail plate occurs almost exclusively in one of the timber members at the time.

From the observations of the specimens after failure, it is visible that the teeth of the double-sided nail plates are bent in both members. For specimens with 200 mm long nail plates (series S8 and SA), the teeth were bent to about 30° from their original position (Fig. 20). The angle for the teeth on the upper side of the nail plate was slightly lower than for the teeth on the lower side. The observation was more pronounced for the series S6 with two separated double-sided nail plates of 100 mm length (Fig. 21), where the angle was about 30° for the upper nail plate and 45° for the lower nail plate.

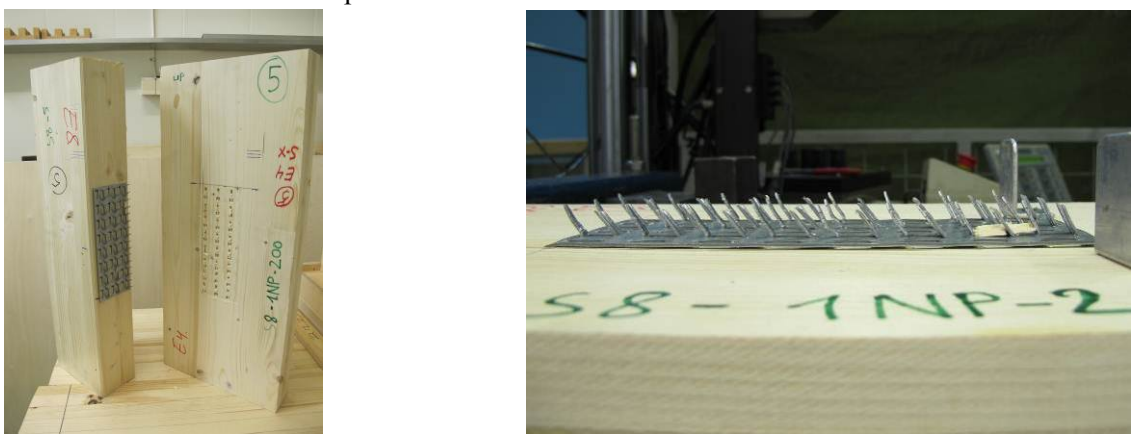

Fig. 20: Specimen with double-sided nail plate 200 mm after failure

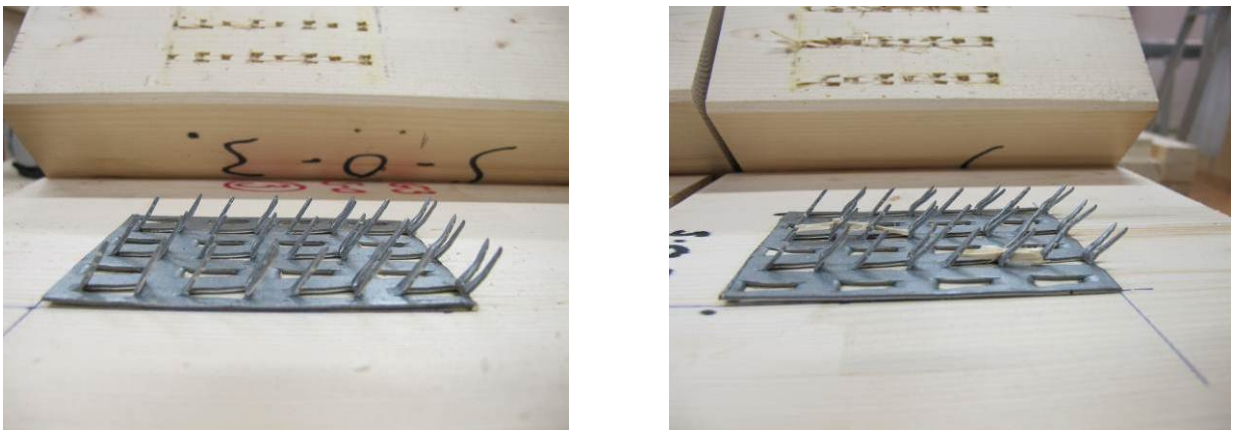

(a) (b)

Fig. 21: Specimen with double-sided nail plates 100 mm after failure – a) upper nail plate – b) lower nail plate

Fig. 22 shows the mean load-slip curve for both test series S6 and S8 up to 6 mm slip. The overall shapes of the load-slip curves are similar. Test series S6 and S8 exhibited similar average ultimate load (+3% for S6). However the slip modulus was lower for S6 (-14%). The difference might come from the position of the nail

plates in the shear plane and from the different compressive forces they are subjected to due to the loading eccentricities generated by the test setup. The rotation of the specimen is prevented at the bottom right by the support and at the top left by the roller support (cf. Fig. 6). For the series S8 the resulting compressive force is concentrated in the nail plate in the middle while in test series S6 it is concentrated on the bottom nail plate. It is observed from the load-slip curves that the results discrepancy was larger in series S6 than is series S8. The coefficient of variation is larger in series S6 for both the maximum load and the slip modulus (cf. Table 4).

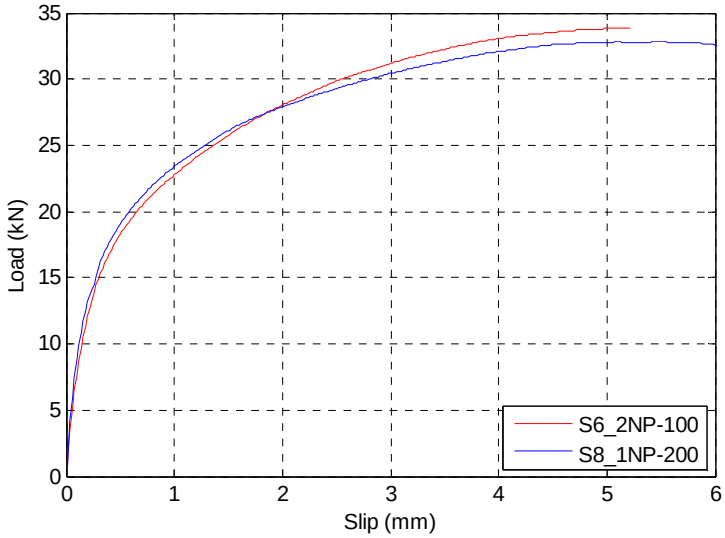

Fig. 22: Mean load-slip curves for test series S6_2NP-100 and S8_1NP-200 up to 6 mm slip

The yield slip evaluations for the joints with double-sided nail plates only give similar results; see Table 5 and Fig. 23. The EN 12512 method is considered appropriate for this evaluation. Despite a higher load-carrying capacity for double-sided nail plate fasteners of 200 mm length than for the tested inclined screws, the nail plate fasteners exhibit a low yield slip, below 0.4 mm with all methods. The connection plasticises significantly after 50 % of the maximum load. The double-sided nail plates connectors can be considered as more plastic than the inclined screws. Observing the load-slip curve before the yield slip, it can be noted that the fasteners actually plasticises from the beginning and that there is no real linear regime as it can be observed for the inclined screws. This may be explained by the fact that the dowel action on teeth of the double-sided nail plates is mobilised already for low displacements.

The double-sided nail plates fasteners plasticise slowly and exhibit a relatively high slip at maximum load, above 5 mm, see Table 4, compared with the inclined screws. The ductility ratio for the definition according to expressions (1) and (2) is therefore high for this type of connector (cf. Table 5).

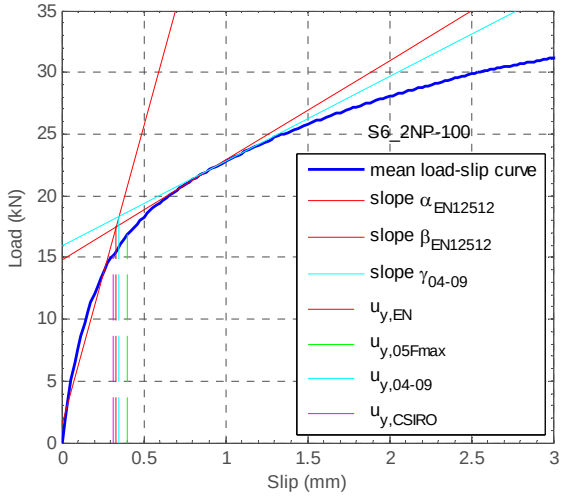

(a)

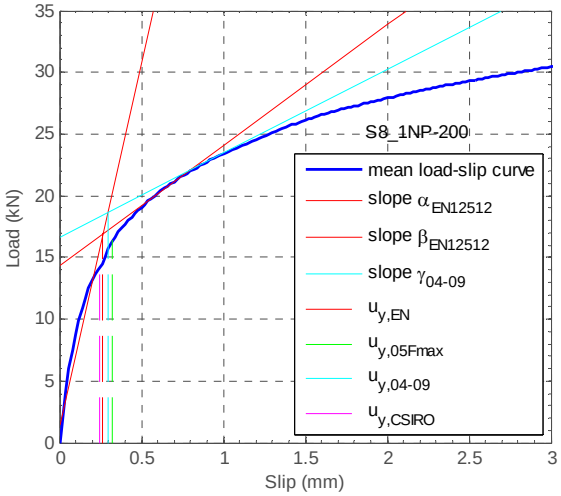

(b)

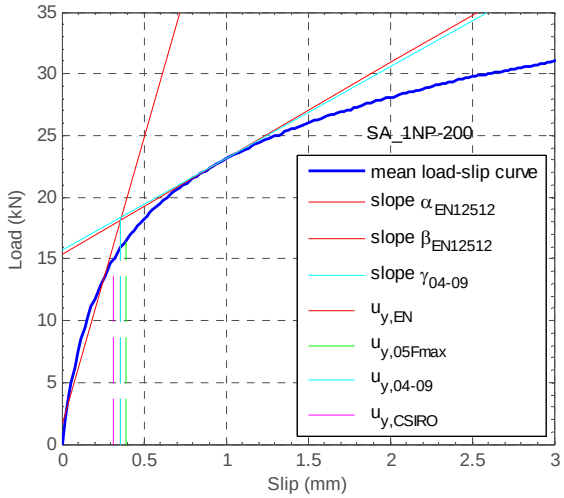

(c)

Fig. 23: Evaluation of the yield slip on the mean load-slip curve, (a) S6, (b) S8, (c) SA

3.4. Test series with double-sided nail plates and inclined screws (S3, S4, S5, S7)

3.4.1. Double-sided nail plate positioned in the centre (S3, S4, S7)

A combination of double-sided nail plates (200 mm) and inclined screws of different diameters, 6.5 and 8.2 mm was used in series S3 and S4, respectively. Double-sided nail plates with length 100 mm were used with two screws of 6.5 mm diameter in series S7. In all cases the contribution of both fasteners types is significant. The ultimate load and the slip modulus significantly increase compared to the joints with nail plates only. The slip at ultimate load, u_{max}, is in-between the values observed for joints with screws only and double-sided nail plates only, with 3.5 mm, 4.2 mm and 2.8 mm for series S3, S4, and S7 respectively.

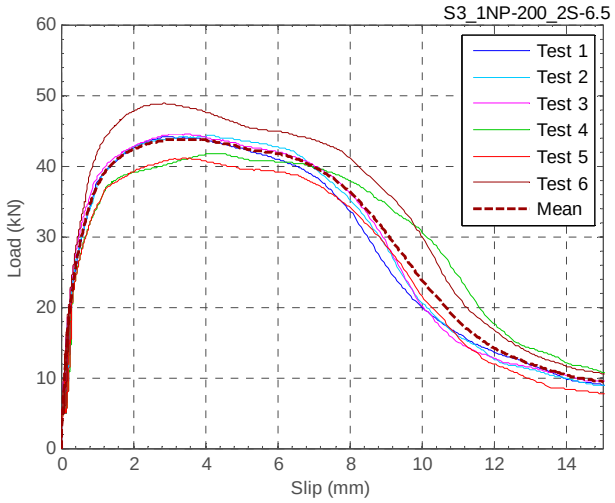

Fig. 24: Load-slip curves - S3_1NP-200/2S-6.5

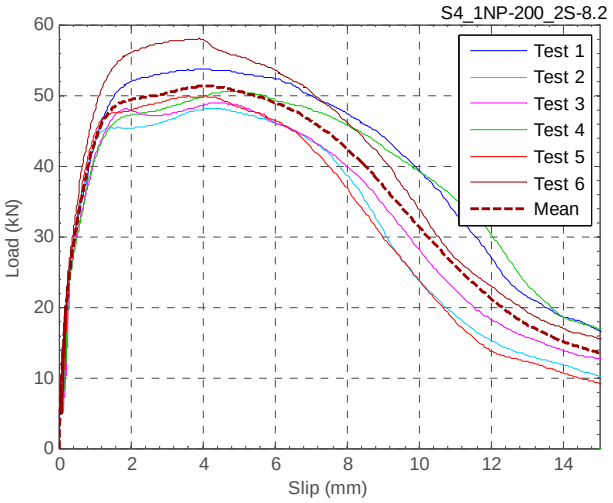

Fig. 25: Load-slip curves - S4_1NP-200/2S-8.2

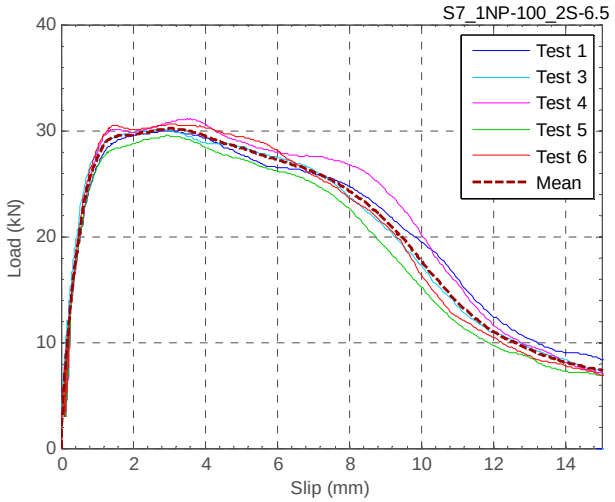

Fig. 26: Load-slip curves - S7_1NP-100/2S-6.5

The behaviour of the joints with double-sided nail plates and inclined screws combined is the superposition of the behaviour of each fastener type taken individually with respect to the applied displacement. Below an applied displacement of 2 mm, the contribution of the screw is visibly added to the contribution of the double-sided nail plates. The withdrawal of the screw occurs between 1.5 and 2 mm slip and can be observed on the load-slip curves. Once the withdrawal of the screw is initiated, the double-sided nail contributes compensates the strength loss from the screws and the overall capacity remains almost equal up to about 4 mm slip. After the ultimate load, the withdrawal of the screws continues to develop and the double-sided nail plate strength

start to significantly decreases. The resulting load-slip curve is a gradually descending slope until 12 mm slip. The reserve capacity between 12 mm and 15 mmm slip is mostly provided by the inclined screws. At the end of the test, the members are not totally separated due to the presence of the screws but a gap of 10 to 20 mm between the members has developed and the double-sided nail plate is fully withdrawn from one side, see Fig. 27.

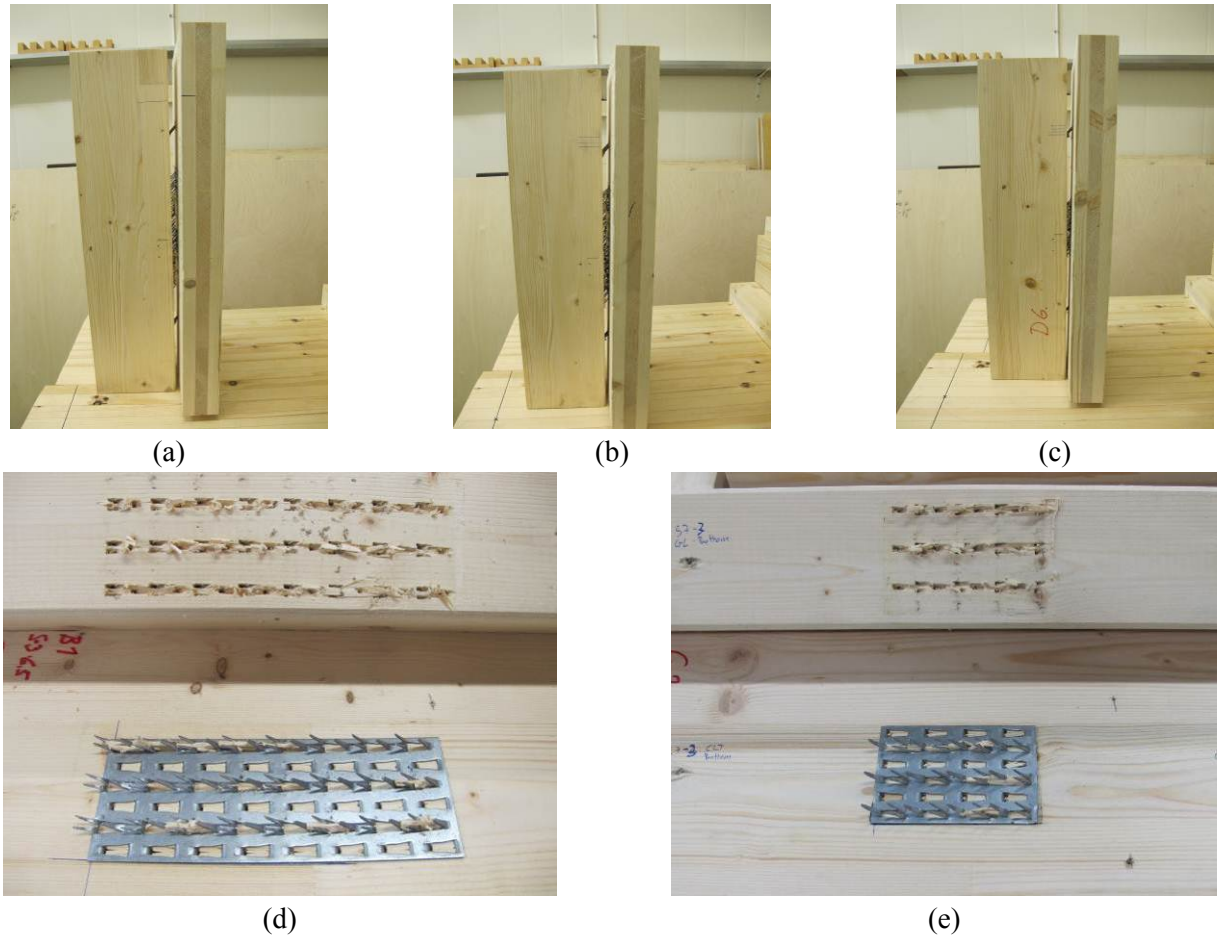

(a) (b) (c)

(d) (e)

Fig. 27: Specimens with combined screw and double-sided nail plates after failure, (a) and (d) S3, (b) S4, (c) and (e) S7

3.4.2. Screw positioned in the centre (S5)

Tests with two double-sided nail plates of 100 mm length placed on each side of an inclined screw were performed to evaluate the effect of the configuration of the shear tests setup and to study different combinations with fewer screws. A combination of two nail plates of 100 mm combined with one screw of 6.5 mm diameter was tested in test series S5, see Fig. 28.

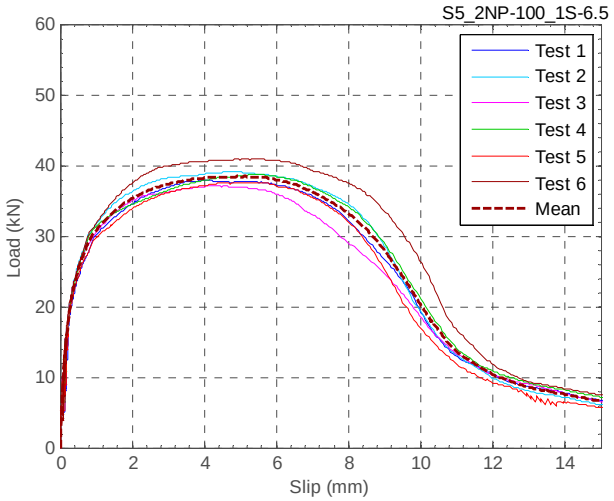

Fig. 28: Load-slip curves - S5_2NP-100_1S-6.5

The maximum load in series S5 was higher than in series S6, but lower than the sum of the load-carrying of the double-sided nail plate and the screw individually. However the slip modulus was increased to a level largely exceeding the sum of the stiffness of each fastener taken individually. This high value might be due to the configuration of the joint and test setup (position of the double-sided nail plate) as well as due to the screw contribution. The calculation method for the slip modulus in EN 26891 [2] may also be responsible for this high value.

The slip modulus k_s of series S5 (2NP-100_1S-6.5) is actually higher than the slip modulus observed for series S3 (1NP-200_2S-6.5) with 80.8 kN/mm and 72.2 kN/mm, respectively, despite the fact that there is one screw in S5 and two screws in S3. This difference between the two series can be partly explained by the method used to evaluate the slip modulus from the load-slip curve. In EN 26891, the slip modulus k_s is calculated according using expression (6).

$$k_s = \frac{0.4 \cdot F_{est}}{v_{i,mod}} \tag{6}$$

with

$$v_{i,mod} = \frac{4}{3}\left(v_{04} - v_{01}\right) \tag{7}$$

and

v_{01} slip at the load $0.1 \cdot F_{est}$

v_{04} slip at the load $0.4 \cdot F_{est}$

F_{est} estimated failure load for the test

The estimated failure loads for series S3 and S5 were different, 50 kN and 40 kN, respectively, see

Table 3. This load is governing the loading procedure and the slip modulus calculation. Evaluating the slip modulus considering the actual mean failure load F_{max} instead of F_{est} gives to slip modulus values of 84.84 kN/mm and 79.67 kN/mm, for series S5 and S3, respectively. The difference between the two series remains but is lower than when considering the estimated failure load for the evaluation.

After failure, the angle of the bent nails in the nail plates was different at the top and at the bottom of the specimen (Fig. 30). At the bottom of the test specimen, the separation is more restrained than at the top due to the test setup configuration. The force distribution between the top and bottom nail plate might be different, with the bottom nail plate having probably a greater contribution.

Fig. 29: Specimens of test series S5 after failure

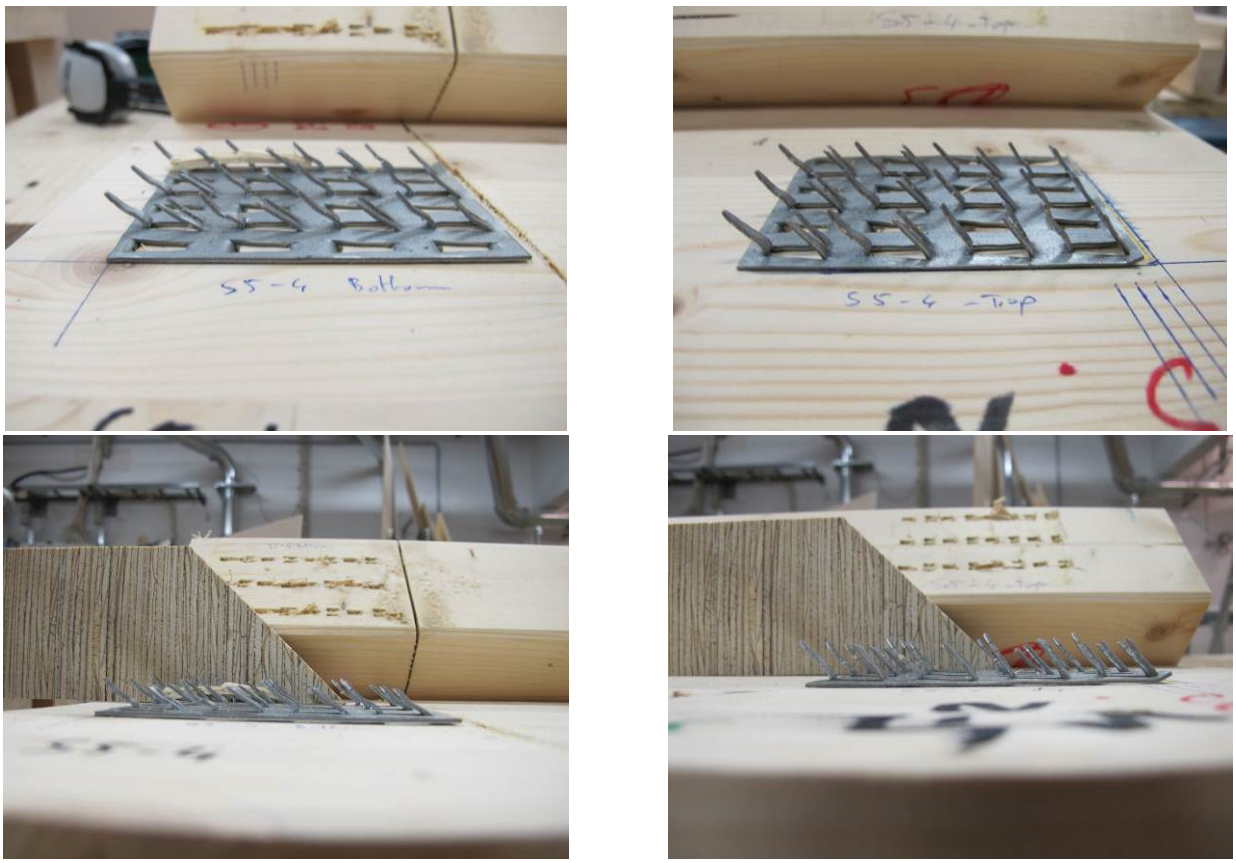

(a) (b)

Fig. 30: Double-sided nail plates 100 mm after failure in series S5 – a) lower nail plate – b) upper nail plate

3.4.3. Yield slip for combined joints

The evaluation of the yield slip for joints with different fastener types combined provides values that do not necessarily lie between the values obtained for the fasteners taken individually, see Fig. 31. The reason for that is that the fasteners in the joint yield individually for different magnitude of applied displacement.

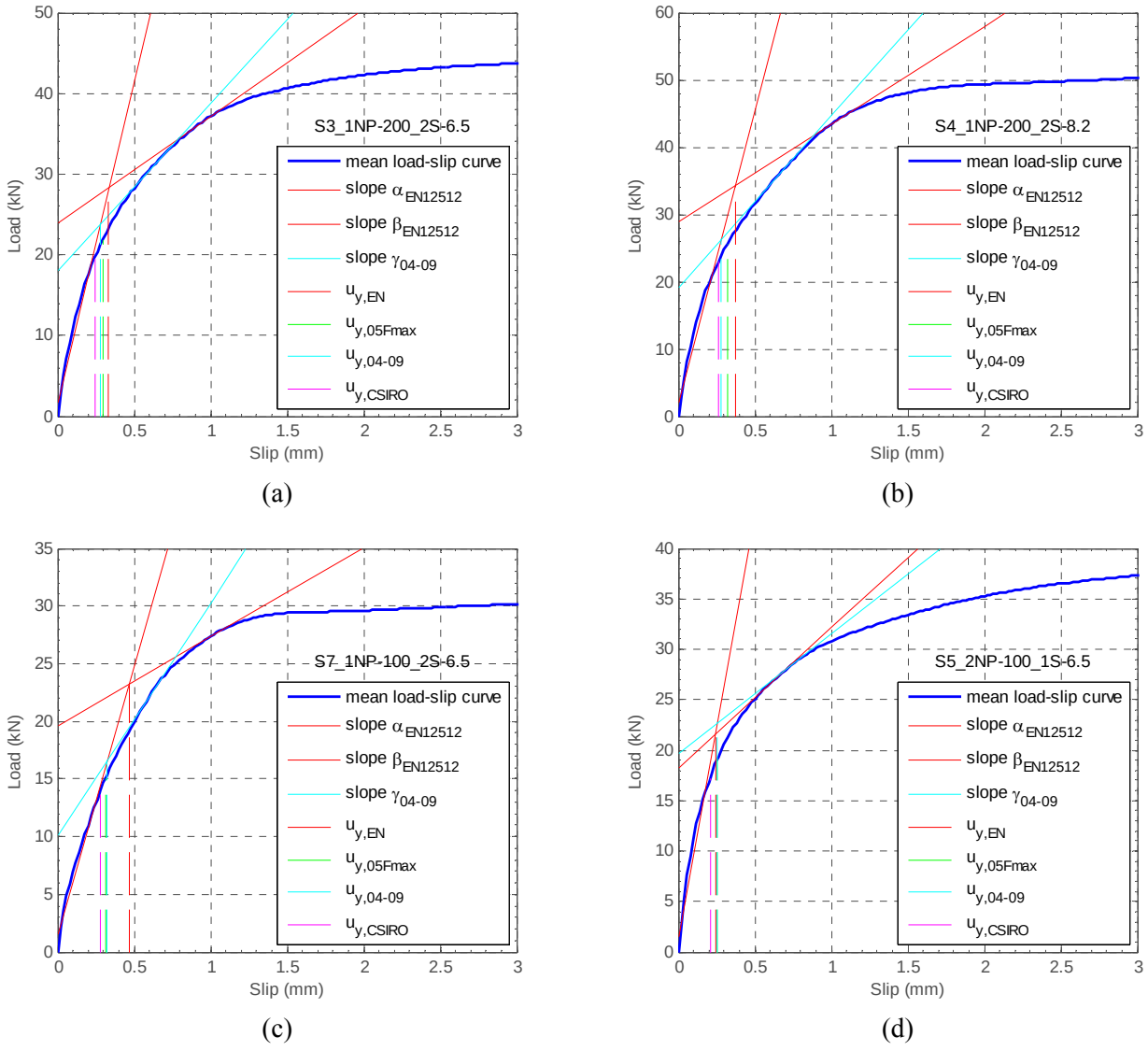

Fig. 31: Evaluation of the yield displacement on the mean load-slip curve, (a) S3, (b) S4, (c) S7, (d) S5

Series S3 and S4 have a similar behaviour and the yield slip evaluations are similar, all below 0.4 mm. Series S7 is made with two screws and a small double-sided nail plate (100 mm long), therefore the influence of the screw is more important than for series S3 and it can be observed that the yield slip according to the EN 12512 method is, as for series S1 and S2, higher than the values obtained with other methods.

4. Comparison between test series

In this section, a comparison table and comparison plots between different test series, one of the aims of this test program being to study the combination effect of fasteners of different types in a joint.

Table 6: Comparison between test results for combined joints and summed values from results on single fastener types

			$F_{max,test}$	$k_{s,test}$	Sum of single fasteners results	$F_{max,sum}$	$k_{s,sum}$	$\frac{F_{max,sum}}{F_{max,test}}$	$\frac{k_{s,sum}}{k_{s,test}}$
			kN	kN/mm		kN	kN/mm	[-]	[-]
Joints with single fastener types	**S1**	**2 S-6.5**	16.09	19.40	-	-	-	-	-
	S2	**2 S-8.2**	22.78	25.42	-	-	-	-	-
	S6	**2 NP-100**	33.94	45.59	-	-	-	-	-
	S8	**1 NP-200**	32.93	53.60	-	-	-	-	-
Joints with combined fasteners	**S3**	**1 NP-200 2 S-6.5**	44.08	72.18	S1 + S8	49.01	73.00	1.11	1.01
	S4	**1 NP-200 2 S-8.2**	51.54	85.00	S2 + S8	55.70	79.02	1.08	0.93
	S5	**2 NP-100 1 S-6.5**	38.54	80.77	$\frac{1}{2}$ S1 + S6	41.99	55.28	1.09	0.68
	S5$_{(S8)}$ [2)]	**2 NP-100 1 S-6.5**	38.54	80.77	$\frac{1}{2}$ S1 + S8	40.97	63.30	1.06	0.78
	S7	**1 NP-100 2 S-6.5**	30.07	46.94	S1 + $\frac{1}{2}$ S8	32.55	46.20	1.08	0.98

- Subscripts "sum" and "test" denote values obtained by summation and from test results, respectively. Note that values for test series S1 and S6 were obtained from a load controlled test.
- $S5_{(S8)}$ denotes the comparison of the test results of series S5 considering the results of series S8 instead of S6

Table 6 presents values for the maximum load $F_{max,sum}$ and slip modulus $k_{s,sum}$ of combined joints obtained by summation of tests results where only one type of fastener was used. These values are calculated using the mean values for the load-carrying capacity $F_{max,test}$ and slip modulus $k_{s,test}$ of test series with one fastener type (S1, S2, S6, S8) and they are compared with the mean values of the test results for the combined joints (S3, S4, S5 and S7).

It is observed that the slip modulus can conservatively be estimated by using the superposition principle, i.e. by summing the values from the tests on single fasteners, while, as expected, the load-carrying capacity is over-estimated using this method by up to 11 %. Depending on the difference in the load-slip characteristics of the two types of fasteners, especially concerning the difference in u_{max} values, a lower value than the sum of the two individual maximum values needs to be used for estimating the load-carrying capacity of the combined joints. According to these test results, a reduction factor of 0.9 seems reasonable to apply. The comparative values in the last two columns in Table 6 are conservative if they are less than one (< 1).

Fig. 32 is made based on the same principle as Table 6 where the load-slip curves for the combined joints S3, S4, S5 and S7 are compared with the load-slip curves made up from superposition of the load-slip curves for the matching single shear connector types (S1, S2 and S8). All the curves presented are mean curves together with curves corresponding to ± the standard deviation (noted σ) for each data point of the mean curves. For S5

(cf Fig. 32c), the load-slip curve from series S8 was used instead of S6 in order to present data up to 15 mm slip.

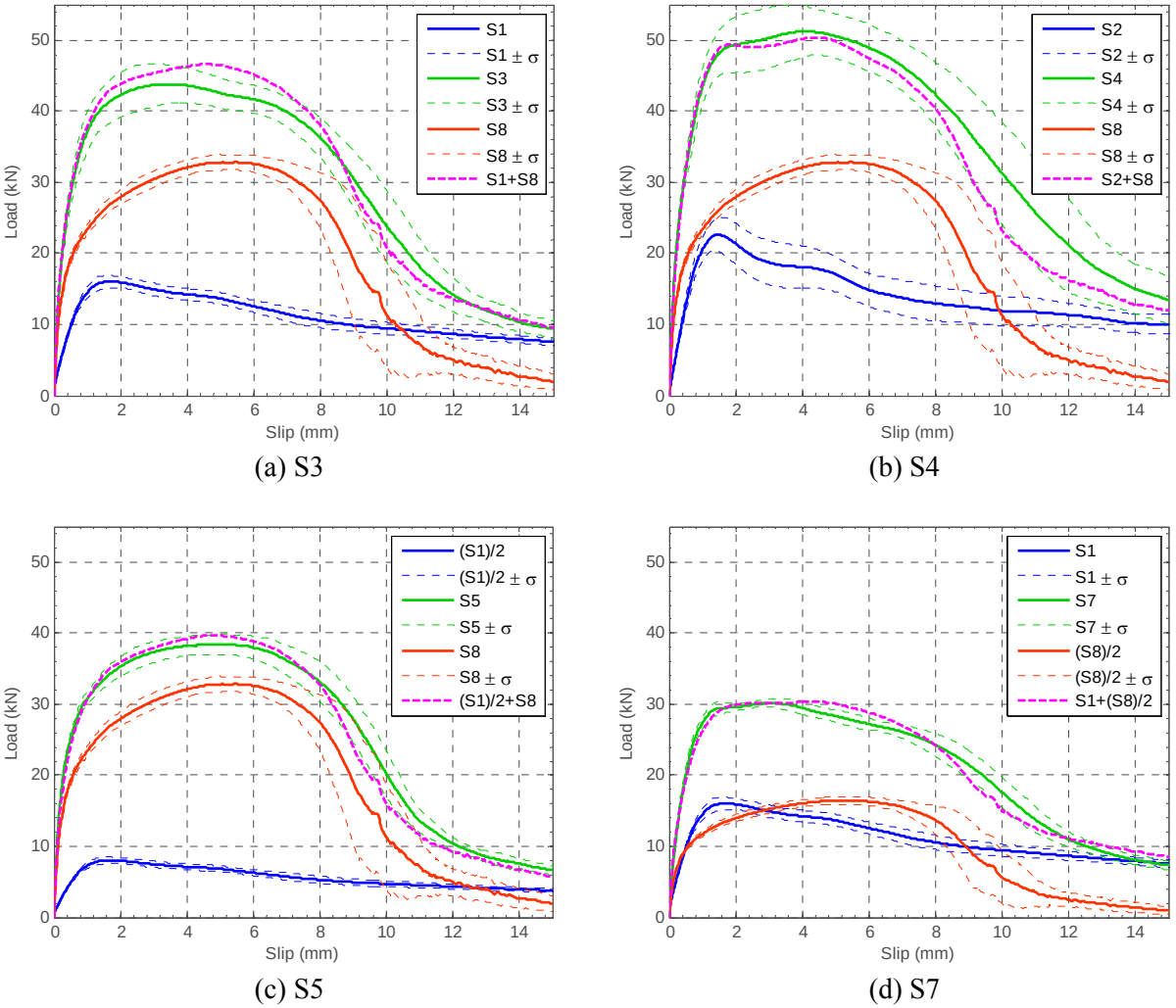

(a) S3 (b) S4

(c) S5 (d) S7

Fig. 32: Mean load-slip curves for combined joints (a) S3, (b) S4, (c) S5 and (d) S7 compared to superposition of the corresponding single fastener load-slip curves.

The summation plots fit well with the tests results of the combined joint, especially considering the joints with 8.2 mm screws (cf. Fig. 32b). For series with 6.5 mm screws, some difference can be observed between the summation plot and the tests results of series S3. This difference might be due to the fact that the tests were load controlled until failure for the test series S1. This leads to a rapid increase of the loading rate after ultimate load is reached. It can be argued that the observed loads might therefore be higher than if the test would have been displacement controlled.

5. Discussion

Joints with multiple fasteners of different type can behave differently. The initial slip modulus, the slip at ultimate load and the post peak behaviour have to be considered in order to ensure that the effect of both fasteners can be considered simultaneously. The behaviour of joints with combined connectors depends on the shape of the curves of the individual fasteners and how compatible they are.

It is rather straightforward to predict the behaviour of a joint with combined fasteners of different nature when the connectors have similar type of behaviours. In terms of ultimate load capacity, the prediction is easier if both connectors reach their maximum load-carrying capacity for the same slip value. Unless there is a strengthening effect due to the combination of the fasteners, the ultimate load of the combined joint will not exceed the sum of the capacities of the fasteners taken individually.

In the present case of a combination of double-sided nail plates with inclined self-tapping screws, the order of magnitude of the slip modulus and the values observed for the load-carrying capacity are such that both fasteners contributions should be considered in the joint design.

However, it should be noted that inclined screws have a relatively low load-carrying capacity compared to double-sided nail plate of 200 mm length but have at the same time a relatively high stiffness. This has for consequence that the screws reach their maximum load-carrying capacity for an applied slip which is lower than for the double-sided nail plates. In addition, the post peak behaviour of the screws is not a plateau as it can be the case for vertical screws and the strength loss after the maximum load is significant. Therefore, the ultimate load capacity of the combined joint is less than the sum of the ultimate load of the screws and double-sided nail plates taken separately.

In order to evaluate precisely the total ultimate load capacity of the joint, the whole load-slip curve for each fastener is necessary. An estimation of the load-slip curve of the combined fasteners in the joint can be obtained by superposition of the individual curves for each fastener.

Based on the results on inclined screws joint in published by Tomasi et al. [15] it may be possible to propose a configuration of the joint where the slip at ultimate load is the same for screws and the double-sided nail plates. This configuration could be more predictable in terms of ultimate load capacity. A screw angle of 15° to 30° perpendicular to the shear plane would give for the screw a slip at maximum load close to 5 mm and therefore a more compatible behaviour with the one of the double-sided nail plates. However, the slip modulus of the overall combined joint with this proposed configuration would less benefit from the contribution of the screw in terms of stiffness than with a screw angle of 45° where the stiffness is the highest.

6. Conclusions

Double-sided nail plate fasteners exhibit an appropriate behaviour as mechanical fasteners for shear load transfer and may be used as the main shear connector for timber to timber layer composite beam elements provided that possible separation forces perpendicular to the shear plane are counteracted.

The most important factors for the combination of mechanical fasteners of different kinds are the compatibility of the load-slip curves in the linear range (evaluation of the yield slip) and to know for which slip value the maximum load is reached. If the maximum load of different fasteners is obtained for the same slip value, then the total capacity might be close the sum of the capacity of the fasteners taken individually, otherwise it can be significantly lower.

The combination of double-sided punched metal plate fasteners and inclined self-tapping screws may be used, where the screws are intended to counteract the possible separation forces and provide additional strength and stiffness to the joint with respect to the shear forces. The design of such combined joint with respect to the load-carrying capacity should be done with caution as the fasteners reach their maximum load for different applied displacement. A lower capacity that the sum the respective load-carrying capacities of the individual fasteners should be used. Concerning the slip modulus of the combined joint, the design may be done by summing the slip modulus of the double-sided nail plates and of the screws.

7. Acknowledgements

The centre for Lean Wood Engineering, the Swedish governmental agency for innovation systems (VINNOVA), Stora Enso Timber, the County Administrative Board in Norrbotten under Grant number 303-2602-13 (174311); the Regional Council of Västerbotten under Grant number REGAC-2013-000133 (00179026); and the European Union's Structural Funds - The Regional Fund under Grant number 2013-000828 (174106) are acknowledged for their financial support to this research.
Ari Kevarinmäki is acknowledged for his comments and assistance for carrying out the tests at VTT Expert Services laboratories in Finland. Sepa Oy and SFS Intec are acknowledged for providing the mechanical fasteners used in this test program.

Appendices

Appendix A. Load-slip curves of test series S1, S2 and S7 including discarded tests

A1. Test series S1_2S-6.5

In the report test specimens 1 and 2 were not considered due to errors of assembly of the specimens. The load-slip curves for the full test series are presented here, including results for Test 1 and Test 2. Due to the small size of the specimens and error the assembly, a significant gap between the members was introduced during the screwing, resulting in a severe reduction of the joint stiffness compared with the rest of the series.

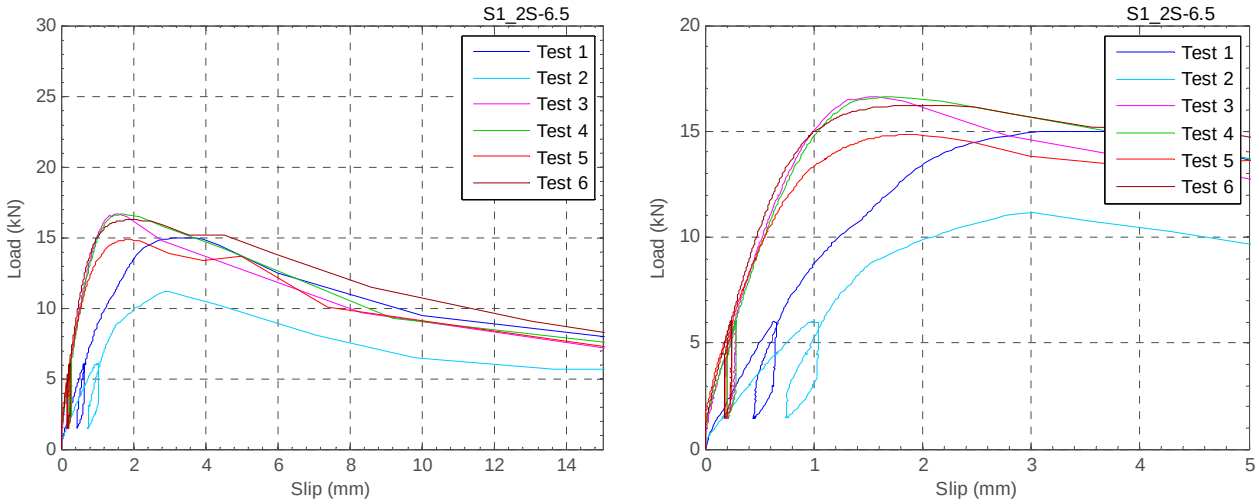

Fig. A-1: Load-slip curves - S1_2S-6.5 including discarded tests

A2. Test series S2_2S-8.2

In the report test specimens 1 and 5 were not considered due to errors of assembly of the specimens. The load-slip curves for the full test series are presented here including results for Test 1 and Test 5. Due to the small size of the specimens and error the assembly, a significant gap between the members was introduced during the screwing, resulting in a severe reduction of the joint stiffness compared with the rest of the series.

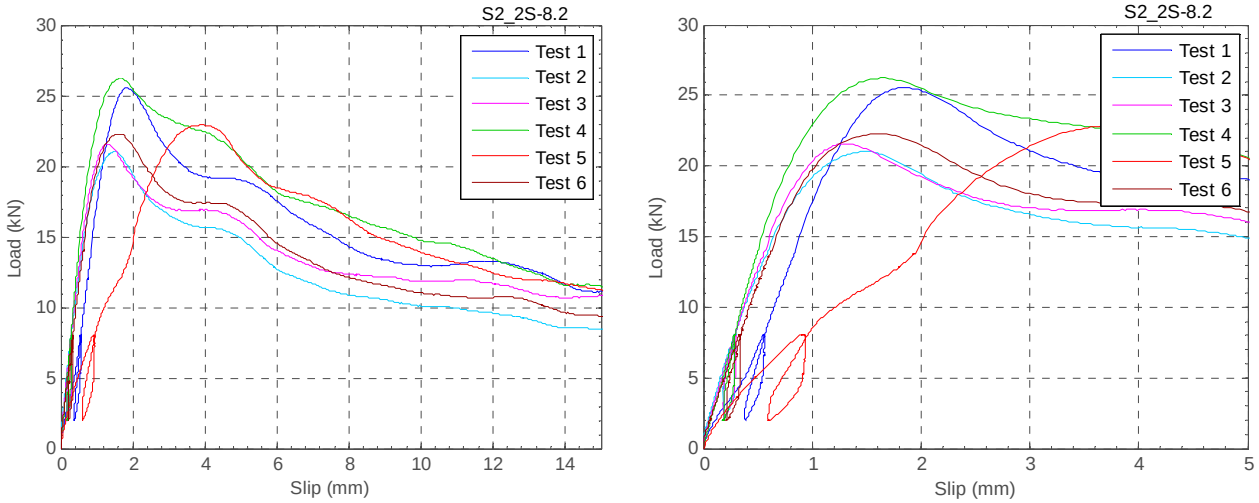

Fig. A-2: Load-slip curves – S2_2S-8.2 including discarded tests

A3. Test series S7_1NP-100_2S-6.5

The test specimen 2 was not considered for the creation of the mean load slip curve in the test report due to its strange post peak behaviour. The test results for this specimen were however considered

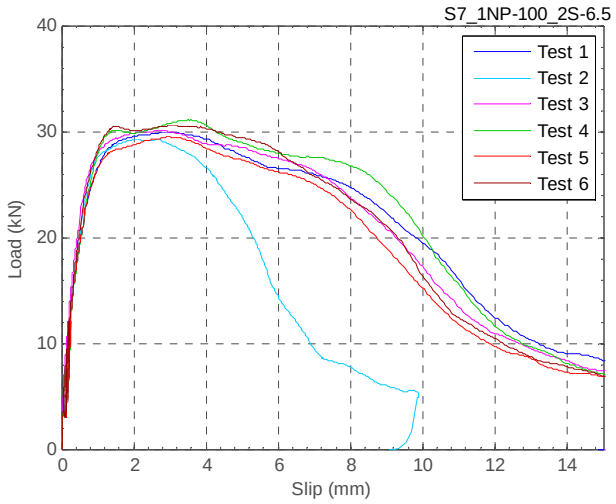

Fig. A-3: Load-slip curves – S7_1NP-100_2S-6.5 including discarded tests

Appendix B. Tables of test results

Table B-1: Detailed test results - Test series S1_2S-6.5

Test Series	S1_2S-6.5							
Test specimen		**3**	**4**	**5**	**6**	**Mean**	**St.dev**	**CoV (%)**
F_{est}	[kN]	15	15	15	15			
F_{04}	[kN]	6	6	6	6			
F_{01}	[kN]	1.5	1.5	1.5	1.5			
n_s		2	2	2	2			
d	[mm]	6.5	6.5	6.5	6.5			
v_{01}	[mm]	0.037	0.025	0.008	0.023	0.023	0.012	50.647
v_{04}	[mm]	0.265	0.281	0.242	0.237	0.256	0.020	7.933
v_{14}	[mm]	0.273	0.286	0.248	0.241	0.262	0.021	8.020
v_{11}	[mm]	0.204	0.208	0.198	0.181	0.198	0.012	6.064
v_{21}	[mm]	0.180	0.203	0.193	0.177	0.188	0.012	6.412
v_{24}	[mm]	0.275	0.282	0.253	0.241	0.262	0.019	7.329
$v_{0,6}$	[mm]	0.523	0.544	0.454	0.457	0.494	0.046	9.274
$v_{0,8}$	[mm]	0.796	0.824	0.750	0.714	0.771	0.049	6.339
v_{max}	[mm]	1.592	1.712	1.850	1.977	1.783	0.167	9.375
v_f	[mm]	4.371	5.361	6.159	6.874	5.691	1.076	18.900
F_{max}	[kN]	16.640	16.654	14.837	16.212	16.086	0.857	5.330
F_{max}/n_s	[kN]	8.320	8.327	7.419	8.106	8.043	0.429	5.330
$v_{i,mod}$	[mm]	0.304	0.341	0.311	0.286	0.311	0.023	7.433
v_s	[mm]	-0.039	-0.061	-0.070	-0.049	-0.055	0.013	-24.523
v_e	[mm]	0.109	0.105	0.073	0.083	0.092	0.017	18.696
k_i	[kN/mm]	22.657	21.390	24.819	25.305	23.543	1.839	7.813
k_s	[kN/mm]	19.733	17.590	19.267	21.007	19.399	1.413	7.284
$v_{i,mod}$-v_{24}	[mm]	0.029	0.059	0.059	0.045	0.048	0.014	29.309
Specific slip values and ductility evaluation								
$u_{y,EN}$	[mm]	0.743	0.788	0.536	0.628	0.674	0.114	16.891
$u_{max} = v_{max}$	[mm]	1.592	1.712	1.850	1.977	1.783	0.167	9.375
$u_f = v_f$	[mm]	4.371	5.361	6.159	6.874	5.691	1.076	18.900
$D_f = u_f / u_{y,EN}$	[-]	5.885	6.806	11.497	10.939	8.782	2.847	32.420
$D_u = u_{max} / u_{y,EN}$	[-]	2.143	2.173	3.452	3.146	2.729	0.671	24.578
$D_{uy} = u_{max} - u_{y,EN}$	[mm]	0.849	0.924	1.314	1.349	1.109	0.259	23.351
$D_{fy} = u_f - u_{y,EN}$	[mm]	3.628	4.573	5.623	6.246	5.018	1.155	23.023
$D_{fu} = u_f - u_{max}$	[mm]	2.779	3.649	4.309	4.897	3.909	0.909	23.266
$u_{y,05Fmax}$	[mm]	0.412	0.427	0.343	0.356	0.384	0.041	10.746
$u_{y,04\text{-}09}$	[mm]	0.446	0.481	0.346	0.413	0.422	0.058	13.696
$u_{y,CSIRO}$	[mm]	0.387	0.399	0.292	0.333	0.353	0.050	14.030
$\rho_{g,\omega}$	[kg/m^3]	454	464	434	473	456	16.6	3.6
$\rho_{g,0,\omega}$	[kg/m^3]	404	413	389	421	407	13.5	3.3
ω_g	[%]	12	12	12	13	12	0.4	3.0
$\rho_{c,\omega}$	[kg/m^3]	483	465	433	501	471	28.9	6.1
$\rho_{c,0,\omega}$	[kg/m^3]	430	413	385	448	419	27.1	6.5
ω_c	[%]	12	13	13	12	12	0.4	3.3

Table B-2: Detailed test results - Test series S2_2S-8.2

Test Series	S2_2S-8.2							
Test specimen		**2**	**3**	**4**	**6**	**Mean**	**St.dev**	**CoV (%)**
F_{est}	[kN]	20	20	20	20			
F_{04}	[kN]	8	8	8	8			
F_{01}	[kN]	2	2	2	2			
n_s		2	2	2	2			
d	[mm]	8.2	8.2	8.2	8.2			
v_{01}	[mm]	0.047	0.060	0.068	0.062	0.059	0.009	15.399
v_{04}	[mm]	0.286	0.290	0.282	0.329	0.297	0.022	7.400
v_{14}	[mm]	0.293	0.297	0.289	0.341	0.305	0.024	7.954
v_{11}	[mm]	0.188	0.190	0.191	0.222	0.198	0.016	8.118
v_{21}	[mm]	0.180	0.185	0.187	0.217	0.192	0.017	8.752
v_{24}	[mm]	0.296	0.292	0.291	0.342	0.305	0.025	8.187
$v_{0,6}$	[mm]	0.517	0.512	0.565	0.589	0.546	0.038	6.880
$v_{0,8}$	[mm]	0.769	0.740	0.848	0.839	0.799	0.053	6.659
v_{max}	[mm]	1.527	1.301	1.669	1.648	1.536	0.169	10.978
v_f	[mm]	2.844	2.788	4.862	3.131	3.406	0.982	28.834
F_{max}	[kN]	21.024	21.592	26.227	22.265	22.777	2.355	10.341
F_{max}/n_s	[kN]	10.512	10.796	13.114	11.133	11.389	1.178	10.341
$v_{i,mod}$	[mm]	0.319	0.307	0.285	0.357	0.317	0.030	9.540
v_s	[mm]	-0.033	-0.016	-0.003	-0.028	-0.020	0.013	-66.567
v_e	[mm]	0.147	0.142	0.134	0.163	0.147	0.012	8.171
k_i	[kN/mm]	28.021	27.584	28.349	24.289	27.061	1.874	6.925
k_s	[kN/mm]	25.115	26.100	28.059	22.400	25.418	2.355	9.266
$v_{i,mod}$-v_{24}	[mm]	0.023	0.015	-0.006	0.015	0.012	0.012	105.259
Specific slip values and ductility evaluation								
$u_{y,EN}$	[mm]	0.721	0.734	0.811	0.911	0.794	0.087	10.987
$u_{max} = v_{max}$	[mm]	1.527	1.301	1.669	1.648	1.536	0.169	10.978
$u_f = v_f$	[mm]	2.844	2.788	4.862	3.131	3.406	0.982	28.834
$D_f = u_f / u_{y,EN}$	[-]	3.943	3.799	5.997	3.437	4.294	1.155	26.903
$D_u = u_{max} / u_{y,EN}$	[-]	2.117	1.773	2.058	1.809	1.939	0.174	8.960
$D_{uy} = u_{max} - u_{y,EN}$	[mm]	0.806	0.567	0.858	0.737	0.742	0.127	17.070
$D_{fy} = u_f - u_{y,EN}$	[mm]	2.123	2.054	4.052	2.220	2.612	0.962	36.829
$D_{fu} = u_f - u_{max}$	[mm]	1.317	1.487	3.194	1.483	1.870	0.886	47.363
$u_{y,05Fmax}$	[mm]	0.405	0.409	0.466	0.474	0.438	0.037	8.384
$u_{y,04\text{-}09}$	[mm]	0.459	0.451	0.558	0.687	0.539	0.110	20.420
$u_{y,CSIRO}$	[mm]	0.386	0.393	0.461	0.477	0.429	0.046	10.808
$\rho_{g,\omega}$	[kg/m^3]	437	491	468	451	462	23.0	5.0
$\rho_{g,0,\omega}$	[kg/m^3]	386	439	416	402	411	22.5	5.5
ω_g	[%]	13	12	12	12	12	0.7	5.3
$\rho_{c,\omega}$	[kg/m^3]	458	432	450	494	459	26.2	5.7
$\rho_{c,0,\omega}$	[kg/m^3]	408	384	401	441	408	24.2	5.9
ω_c	[%]	12	13	12	12	12	0.2	2.0

Table B-3: Detailed test results - Test series S3_1NP-200/2S-6.5

Test Series	S3_1NP-200_2S-6.5								
Test specimen		**1**	**2**	**3**	**4**	**5**	**6**	**Mean**	**St.dev**	**CoV (%)**
F_{est}	[kN]	50	50	50	50	50	50			
F_{04}	[kN]	20	20	20	20	20	20			
F_{01}	[kN]	5	5	5	5	5	5			
A	[mm^2]	14400	14400	14400	14400	14400	14400			
t_i	[mm]	1.3	1.3	1.3	1.3	1.3	1.3			
n_s		2	2	2	2	2	2			
d	[mm]	6.5	6.5	6.5	6.5	6.5	6.5			
v_{01}	[mm]	0.039	0.038	0.037	0.044	0.043	0.034	0.039	0.004	9.394
v_{04}	[mm]	0.254	0.239	0.219	0.290	0.277	0.217	0.250	0.030	11.996
v_{14}	[mm]	0.273	0.254	0.231	0.305	0.299	0.231	0.265	0.032	12.224
v_{11}	[mm]	0.132	0.118	0.103	0.145	0.143	0.102	0.124	0.019	15.450
v_{21}	[mm]	0.128	0.115	0.100	0.140	0.140	0.099	0.120	0.019	15.443
v_{24}	[mm]	0.274	0.257	0.233	0.307	0.304	0.230	0.268	0.033	12.475
$v_{0,6}$	[mm]	0.447	0.426	0.381	0.445	0.431	0.450	0.430	0.026	5.999
$v_{0,8}$	[mm]	0.874	0.910	0.801	0.936	0.871	0.819	0.868	0.052	5.930
u_{max}	[mm]	2.864	4.166	3.225	4.243	3.537	2.875	3.485	0.611	17.536
u_f	[mm]	7.698	7.961	8.095	9.253	8.259	8.422	8.281	0.537	6.483
F_{max}	[kN]	44.083	44.268	44.478	41.785	41.026	48.822	44.077	2.730	6.195
F_{max}/A	[N/mm^2]	3.061	3.074	3.089	2.902	2.849	3.390	3.061	0.190	6.195
$v_{i,mod}$	[mm]	0.287	0.268	0.243	0.328	0.313	0.244	0.281	0.035	12.558
v_s	[mm]	-0.033	-0.029	-0.024	-0.038	-0.035	-0.027	-0.031	0.005	-17.538
v_e	[mm]	0.192	0.185	0.175	0.218	0.214	0.174	0.193	0.019	9.956
k_i	[kN/mm]	78.634	83.565	91.158	68.966	72.100	92.014	81.073	9.599	11.840
k_s	[kN/mm]	69.567	74.575	82.237	60.893	63.995	81.808	72.179	8.953	12.404
$v_{i,mod}$-v_{24}	[mm]	0.013	0.012	0.010	0.022	0.009	0.014	0.013	0.005	35.331
Specific slip values and ductility evaluation										
$u_{y,EN}$	[mm]	0.362	0.316	0.308	0.355	0.323	0.372	0.339	0.027	7.935
u_{max}	[mm]	2.864	4.166	3.225	4.243	3.537	2.875	3.485	0.611	17.536
u_f	[mm]	7.698	7.961	8.095	9.253	8.259	8.422	8.281	0.537	6.483
$D_f = u_f / u_{y,EN}$	[-]	21.264	25.202	26.319	26.080	25.576	22.668	24.518	2.063	8.415
$D_u = u_{max} / u_{y,EN}$	[-]	7.910	13.187	10.484	11.959	10.953	7.738	10.372	2.182	21.035
$D_{uy} = u_{max} - u_{y,EN}$	[mm]	2.501	3.850	2.917	3.888	3.214	2.503	3.146	0.622	19.761
$D_{fy} = u_f - u_{y,EN}$	[mm]	7.336	7.646	7.787	8.898	7.936	8.051	7.942	0.530	6.673
$D_{fu} = u_f - u_{max}$	[mm]	4.835	3.795	4.870	5.010	4.722	5.547	4.797	0.570	11.881
$u_{y,05Fmax}$	[mm]	0.311	0.292	0.267	0.322	0.313	0.311	0.303	0.020	6.668
$u_{y,04-09}$	[mm]	0.293	0.273	0.271	0.311	0.275	0.297	0.287	0.016	5.611
$u_{y,CSIRO}$	[mm]	0.257	0.242	0.230	0.267	0.246	0.261	0.250	0.014	5.403
$\rho_{g,\omega}$	[kg/m^3]	464	447	478	455	461	496	467	17.6	3.8
$\rho_{g,0,\omega}$	[kg/m^3]	412	398	425	403	409	440	415	15.6	3.8
ω_g	[%]	12.7	12.2	12.4	12.9	12.7	12.6	12.6	0.3	2.1
$\rho_{c,\omega}$	[kg/m^3]	484	444	455	448	485	424	457	24.0	5.3
$\rho_{c,0,\omega}$	[kg/m^3]	430	393	403	397	429	375	405	21.5	5.3
ω_c	[%]	12.6	12.9	12.8	13.0	13.1	13.0	12.9	0.2	1.4

Table B-4: Detailed test results - Test series S4_1NP-200/2S-8.2

Test Series	S4_1NP-200_2S-8.2								
Test specimen		**1**	**2**	**3**	**4**	**5**	**6**	**Mean**	**St.dev**	**CoV (%)**
F_{est}	[kN]	55	55	55	50	50	50			
F_{04}	[kN]	22	22	22	20	20	20			
F_{01}	[kN]	5.5	5.5	5.5	5	5	5			
A	[mm^2]	14400	14400	14400	14400	14400	14400			
t_i	[mm]	1.3	1.3	1.3	1.3	1.3	1.3			
n_s		2	2	2	2	2	2			
d	[mm]	8.2	8.2	8.2	8.2	8.2	8.2			
v_{01}	[mm]	0.039	0.035	0.038	0.035	0.034	0.034	0.036	0.002	6.131
v_{04}	[mm]	0.229	0.229	0.266	0.226	0.201	0.188	0.223	0.027	12.180
v_{14}	[mm]	0.242	0.242	0.280	0.239	0.212	0.195	0.235	0.029	12.465
v_{11}	[mm]	0.113	0.112	0.132	0.116	0.089	0.084	0.108	0.018	16.771
v_{21}	[mm]	0.108	0.109	0.127	0.112	0.086	0.083	0.104	0.017	15.940
v_{24}	[mm]	0.244	0.248	0.283	0.241	0.212	0.197	0.237	0.030	12.643
$v_{0,6}$	[mm]	0.516	0.401	0.473	0.537	0.431	0.525	0.480	0.055	11.473
$v_{0,8}$	[mm]	0.994	0.773	0.911	0.971	0.753	0.927	0.888	0.102	11.451
u_{max}	[mm]	3.874	4.299	4.417	4.933	3.640	3.893	4.176	0.470	11.257
u_f	[mm]	9.231	8.013	8.165	9.641	7.505	7.943	8.416	0.830	9.863
F_{max}	[kN]	53.738	48.197	48.922	50.513	49.827	58.011	51.535	3.707	7.194
F_{max}/A	[N/mm^2]	3.732	3.347	3.397	3.508	3.460	4.029	3.579	0.257	7.194
$v_{i,mod}$	[mm]	0.253	0.259	0.305	0.255	0.223	0.205	0.250	0.034	13.730
v_s	[mm]	-0.024	-0.029	-0.038	-0.029	-0.022	-0.017	-0.027	0.007	-27.697
v_e	[mm]	0.176	0.179	0.203	0.168	0.166	0.150	0.173	0.018	10.104
k_i	[kN/mm]	96.082	95.935	82.583	88.341	99.502	106.542	94.831	8.413	8.872
k_s	[kN/mm]	87.036	85.072	72.172	78.372	89.824	97.543	85.003	8.868	10.433
$v_{i,mod}$-v_{24}	[mm]	0.009	0.011	0.022	0.015	0.011	0.008	0.013	0.005	40.450
Specific slip values and ductility evaluation										
$u_{y,EN}$	[mm]	0.353	0.310	0.374	0.441	0.365	0.433	0.379	0.050	13.092
u_{max}	[mm]	3.874	4.299	4.417	4.933	3.640	3.893	4.176	0.470	11.257
u_f	[mm]	9.231	8.013	8.165	9.641	7.505	7.943	8.416	0.830	9.863
$D_f = u_f / u_{y,EN}$	[-]	26.187	25.832	21.829	21.880	20.556	18.363	22.441	3.046	13.575
$D_u = u_{max} / u_{y,EN}$	[-]	10.989	13.858	11.810	11.195	9.970	9.000	11.137	1.662	14.923
$D_{uy} = u_{max} - u_{y,EN}$	[mm]	3.521	3.989	4.043	4.492	3.275	3.460	3.797	0.457	12.027
$D_{fy} = u_f - u_{y,EN}$	[mm]	8.879	7.703	7.791	9.201	7.140	7.511	8.037	0.815	10.135
$D_{fu} = u_f - u_{max}$	[mm]	5.357	3.714	3.748	4.708	3.865	4.050	4.240	0.658	15.512
$u_{y,05Fmax}$	[mm]	0.337	0.277	0.326	0.357	0.298	0.361	0.326	0.033	10.200
$u_{y,04\text{-}09}$	[mm]	0.276	0.230	0.272	0.355	0.262	0.328	0.287	0.046	15.983
$u_{y,CSIRO}$	[mm]	0.271	0.224	0.263	0.307	0.249	0.300	0.269	0.031	11.558
$\rho_{g,\omega}$	[kg/m^3]	460	416	462	442	435	492	451	26.3	5.8
$\rho_{g,0,\omega}$	[kg/m^3]	409	370	411	392	387	437	401	23.3	5.8
ω_g	[%]	12.6	12.4	12.4	12.7	12.5	12.5	12.5	0.1	0.8
$\rho_{c,\omega}$	[kg/m^3]	488	436	480	450	476	433	460	23.7	5.2
$\rho_{c,0,\omega}$	[kg/m^3]	431	387	426	399	422	383	408	20.8	5.1
ω_c	[%]	13.2	12.7	12.6	12.6	12.7	12.9	12.8	0.2	1.8

Table B-5: Detailed test results - Test series S5_2NP-100/1S-6.5

Test Series	S5_2NP-100_1S-6.5								
Test specimen		**1**	**2**	**3**	**4**	**5**	**6**	**Mean**	**St.dev**	**CoV (%)**
F_{est}	[kN]	40	40	40	40	40	40			
F_{04}	[kN]	16	16	16	16	16	16			
F_{01}	[kN]	4	4	4	4	4	4			
A	[mm^2]	14400	14400	14400	14400	14400	14400			
t_i	[mm]	1.3	1.3	1.3	1.3	1.3	1.3			
n_s		1	1	1	1	1	1			
d	[mm]	6.5	6.5	6.5	6.5	6.5	6.5			
v_{01}	[mm]	0.033	0.033	0.026	0.031	0.029	0.026	0.030	0.003	11.090
v_{04}	[mm]	0.200	0.169	0.175	0.178	0.188	0.164	0.179	0.013	7.378
v_{14}	[mm]	0.214	0.178	0.184	0.186	0.202	0.176	0.190	0.015	7.822
v_{11}	[mm]	0.104	0.083	0.082	0.089	0.098	0.079	0.089	0.010	11.170
v_{21}	[mm]	0.100	0.080	0.080	0.087	0.096	0.076	0.086	0.010	11.016
v_{24}	[mm]	0.217	0.185	0.185	0.190	0.204	0.179	0.193	0.014	7.420
$v_{0,6}$	[mm]	0.432	0.383	0.343	0.393	0.404	0.446	0.400	0.037	9.178
$v_{0,8}$	[mm]	1.028	0.953	0.908	0.928	1.077	1.124	1.003	0.087	8.668
u_{max}	[mm]	4.133	4.628	4.363	5.367	5.394	5.169	4.842	0.541	11.181
u_f	[mm]	8.354	8.627	7.834	8.680	8.349	9.137	8.497	0.434	5.105
F_{max}	[kN]	37.889	39.138	37.118	38.657	37.590	40.874	38.544	1.354	3.513
F_{max}/A	[N/mm^2]	2.631	2.718	2.578	2.685	2.610	2.838	2.677	0.094	3.513
$v_{i,mod}$	[mm]	0.223	0.181	0.198	0.196	0.211	0.185	0.199	0.016	7.952
v_s	[mm]	-0.023	-0.012	-0.023	-0.018	-0.024	-0.021	-0.020	0.004	-21.511
v_e	[mm]	0.151	0.133	0.138	0.133	0.142	0.133	0.138	0.007	5.217
k_i	[kN/mm]	79.861	94.955	91.667	89.888	85.333	97.301	89.834	6.404	7.129
k_s	[kN/mm]	71.765	88.452	80.851	81.522	75.680	86.370	80.773	6.292	7.790
$v_{i,mod}$-v_{24}	[mm]	0.006	-0.004	0.013	0.007	0.007	0.006	0.006	0.005	93.857
Specific slip values and ductility evaluation										
$u_{y,EN}$	[mm]	0.259	0.230	0.226	0.242	0.241	0.273	0.245	0.018	7.317
u_{max}	[mm]	4.133	4.628	4.363	5.367	5.394	5.169	4.842	0.541	11.181
u_f	[mm]	8.354	8.627	7.834	8.680	8.349	9.137	8.497	0.434	5.105
$D_f = u_f / u_{y,EN}$	[-]	32.221	37.561	34.665	35.809	34.680	33.463	34.733	1.849	5.322
$D_u = u_{max} / u_{y,EN}$	[-]	15.939	20.147	19.303	22.140	22.403	18.932	19.811	2.378	12.004
$D_{uy} = u_{max} - u_{y,EN}$	[mm]	3.873	4.398	4.136	5.124	5.153	4.896	4.597	0.539	11.722
$D_{fy} = u_f - u_{y,EN}$	[mm]	8.094	8.398	7.608	8.437	8.109	8.864	8.252	0.422	5.111
$D_{fu} = u_f - u_{max}$	[mm]	4.221	4.000	3.472	3.313	2.956	3.968	3.655	0.485	13.271
$u_{y,05Fmax}$	[mm]	0.282	0.252	0.229	0.255	0.261	0.274	0.259	0.019	7.161
$u_{y,04\text{-}09}$	[mm]	0.273	0.244	0.233	0.277	0.258	0.278	0.261	0.019	7.248
$u_{y,CSIRO}$	[mm]	0.224	0.202	0.188	0.206	0.208	0.227	0.209	0.015	6.966
$\rho_{g,\omega}$	[kg/m^3]	439	433	462	465	455	511	461	27.6	6.0
$\rho_{g,0,\omega}$	[kg/m^3]	390	385	412	411	404	454	409	24.7	6.0
ω_g	[%]	12.7	12.5	12.1	12.9	12.5	12.5	12.5	0.3	2.1
$\rho_{c,\omega}$	[kg/m^3]	426	458	461	469	465	428	451	18.9	4.2
$\rho_{c,0,\omega}$	[kg/m^3]	377	405	409	415	410	378	399	16.8	4.2
ω_c	[%]	13.0	13.2	12.7	13.1	13.3	13.2	13.1	0.2	1.6

Table B-6: Detailed test results - Test series S6_2NP-100

Test Series	S6_2NP-100								
Test specimen		**1**	**2**	**3**	**4**	**5**	**6**	**Mean**	**St.dev**	**CoV (%)**
F_{est}	[kN]	35	35	35	35	35	35			
F_{04}	[kN]	14	14	14	14	14	14			
F_{01}	[kN]	3.5	3.5	3.5	3.5	3.5	3.5			
A	[mm^2]	14400	14400	14400	14400	14400	14400			
t_i	[mm]	1.3	1.3	1.3	1.3	1.3	1.3			
v_{01}	[mm]	0.045	0.037	0.038	0.042	0.041	0.036	0.040	0.003	8.634
v_{04}	[mm]	0.386	0.221	0.284	0.304	0.248	0.237	0.280	0.060	21.524
v_{14}	[mm]	0.440	0.242	0.318	0.340	0.266	0.256	0.310	0.074	23.803
v_{11}	[mm]	0.293	0.125	0.189	0.208	0.114	0.133	0.177	0.068	38.433
v_{21}	[mm]	0.285	0.122	0.185	0.206	0.104	0.131	0.172	0.068	39.445
v_{24}	[mm]	0.448	0.242	0.321	0.345	0.210	0.257	0.304	0.087	28.561
$v_{0,6}$	[mm]	0.875	0.541	0.758	0.855	0.627	0.606	0.710	0.139	19.608
$v_{0,8}$	[mm]	2.119	1.436	1.816	1.874	1.745	1.705	1.783	0.223	12.534
v_{max}	[mm]	5.471	4.595	4.886	5.452	5.488	5.263	5.192	0.371	7.143
v_f	[mm]	5.471	5.233	7.386	8.535	6.595	7.195	6.736	1.245	18.481
F_{max}	[kN]	30.930	34.134	33.488	34.479	35.702	34.917	33.942	1.652	4.868
F_{max}/A	[N/mm^2]	2.148	2.370	2.326	2.394	2.479	2.425	2.357	0.115	4.868
$v_{i,mod}$	[mm]	0.454	0.245	0.328	0.350	0.276	0.268	0.320	0.076	23.848
v_s	[mm]	-0.068	-0.024	-0.044	-0.046	-0.028	-0.031	-0.040	0.016	-40.337
v_e	[mm]	0.207	0.158	0.176	0.181	0.172	0.167	0.177	0.017	9.444
k_i	[kN/mm]	36.269	63.287	49.304	46.001	56.499	59.028	51.731	9.872	19.083
k_s	[kN/mm]	30.824	57.091	42.732	39.977	50.720	52.166	45.585	9.587	21.031
$v_{i,mod}$-v_{24}	[mm]	0.006	0.004	0.007	0.005	0.066	0.011	0.016	0.024	147.403
Specific slip values and ductility evaluation										
$u_{y,EN}$	[mm]	0.369	0.285	0.328	0.389	0.270	0.325	0.328	0.046	14.067
$u_{max} = v_{max}$	[mm]	5.471	4.595	4.886	5.452	5.488	5.263	5.192	0.371	7.143
$u_f = v_f$	[mm]	5.471	5.233	7.386	8.535	6.595	7.195	6.736	1.245	18.481
$D_f = u_f / u_{y,EN}$	[-]	14.826	18.357	22.488	21.919	24.403	22.122	20.686	3.476	16.803
$D_u = u_{max} / u_{y,EN}$	[-]	14.826	16.119	14.877	14.002	20.307	16.182	16.052	2.245	13.988
$D_{uy} = u_{max} - u_{y,EN}$	[mm]	5.102	4.310	4.558	5.063	5.217	4.938	4.865	0.354	7.281
$D_{fy} = u_f - u_{y,EN}$	[mm]	5.102	4.948	7.057	8.145	6.324	6.870	6.408	1.225	19.110
$D_{fu} = u_f - u_{max}$	[mm]	0.000	0.638	2.500	3.083	1.107	1.932	1.543	1.169	75.719
$u_{y,05Fmax}$	[mm]	0.502	0.331	0.427	0.500	0.354	0.373	0.415	0.074	17.921
$u_{y,04-09}$	[mm]	0.387	0.303	0.344	0.382	0.302	0.349	0.344	0.037	10.672
$u_{y,CSIRO}$	[mm]	0.358	0.262	0.317	0.364	0.268	0.293	0.310	0.044	14.144
$\rho_{g,\omega}$	[kg/m^3]	446	422	450	422	424	500	444	30.4	6.8
$\rho_{g,0,\omega}$	[kg/m^3]	394	375	399	376	376	443	394	26.2	6.7
ω_g	[%]	13.2	12.6	12.7	12.2	12.8	13.0	12.7	0.3	2.6
$\rho_{c,\omega}$	[kg/m^3]	368	500	484	432	471	447	450	46.9	10.4
$\rho_{c,0,\omega}$	[kg/m^3]	324	437	426	380	418	390	396	41.3	10.4
ω_c	[%]	13.7	14.3	13.6	13.8	12.8	14.6	13.8	0.6	4.5

Table B-7: Detailed test results - Test series S7_1NP-100/2S-6.5

Test Series	S7_1NP-100_2S-6.5								
Test specimen		**1**	**2**	**3**	**4**	**5**	**6**	**Mean**	**St.dev**	**CoV (%)**
F_{est}	[kN]	30	30	30	30	30	30			
F_{04}	[kN]	12	12	12	12	12	12			
F_{01}	[kN]	3	3	3	3	3	3			
A	[mm^2]	7200	7200	7200	7200	7200	7200			
t_i	[mm]	1.3	1.3	1.3	1.3	1.3	1.3			
n_s		2	2	2	2	2	2			
d	[mm]	6.5	6.5	6.5	6.5	6.5	6.5			
v_{01}	[mm]	0.032	0.033	0.020	0.036	0.039	0.032	0.032	0.007	20.579
v_{04}	[mm]	0.234	0.222	0.188	0.243	0.240	0.220	0.225	0.020	8.955
v_{14}	[mm]	0.245	0.230	0.195	0.250	0.250	0.231	0.233	0.021	8.977
v_{11}	[mm]	0.114	0.103	0.125	0.119	0.119	0.109	0.115	0.008	6.860
v_{21}	[mm]	0.111	0.099	0.121	0.117	0.114	0.105	0.111	0.008	7.410
v_{24}	[mm]	0.244	0.230	0.199	0.251	0.249	0.229	0.234	0.020	8.403
$v_{0,6}$	[mm]	0.442	0.391	0.361	0.480	0.431	0.420	0.421	0.041	9.769
$v_{0,8}$	[mm]	0.760	0.646	0.613	0.782	0.721	0.683	0.701	0.066	9.375
u_{max}	[mm]	2.868	2.041	2.650	3.494	2.947	3.080	2.846	0.484	17.007
u_f	[mm]	8.359	4.699	7.892	8.875	7.647	7.677	7.525	1.461	19.420
F_{max}	[kN]	29.982	29.255	30.030	31.078	29.509	30.581	30.073	0.673	2.238
F_{max}/A	[N/mm^2]	4.164	4.063	4.171	4.316	4.098	4.247	4.177	0.093	2.238
$v_{i,mod}$	[mm]	0.269	0.251	0.225	0.276	0.269	0.251	0.257	0.019	7.306
v_s	[mm]	-0.035	-0.030	-0.037	-0.033	-0.029	-0.030	-0.032	0.003	-10.122
v_e	[mm]	0.175	0.172	0.098	0.177	0.178	0.164	0.161	0.031	19.312
k_i	[kN/mm]	51.282	54.146	63.773	49.408	49.943	54.450	53.834	5.301	9.847
k_s	[kN/mm]	44.535	47.730	53.360	43.489	44.608	47.891	46.935	3.630	7.733
$v_{i,mod}$-v_{24}	[mm]	0.026	0.021	0.026	0.025	0.020	0.022	0.023	0.003	11.911
Specific slip values and ductility evaluation										
$u_{y,EN}$	[mm]	0.474	0.454	0.404	0.563	0.466	0.495	0.476	0.052	11.026
u_{max}	[mm]	2.868	2.041	2.650	3.494	2.947	3.080	2.846	0.484	17.007
u_f	[mm]	8.359	4.699	7.892	8.875	7.647	7.677	7.525	1.461	19.420
$D_f = u_f / u_{y,EN}$	[-]	17.625	10.349	19.550	15.761	16.416	15.502	15.867	3.084	19.436
$D_u = u_{max} / u_{y,EN}$	[-]	6.046	4.495	6.563	6.205	6.325	6.218	5.975	0.745	12.471
$D_{uy} = u_{max} - u_{y,EN}$	[mm]	2.393	1.587	2.246	2.931	2.481	2.584	2.370	0.448	18.885
$D_{fy} = u_f - u_{y,EN}$	[mm]	7.885	4.245	7.488	8.312	7.181	7.182	7.049	1.441	20.445
$D_{fu} = u_f - u_{max}$	[mm]	5.491	2.658	5.242	5.381	4.701	4.598	4.679	1.055	22.544
$u_{y,05Fmax}$	[mm]	0.326	0.294	0.266	0.354	0.322	0.312	0.312	0.030	9.692
$u_{y,04\text{-}09}$	[mm]	0.342	0.292	0.288	0.363	0.342	0.346	0.329	0.031	9.455
$u_{y,CSIRO}$	[mm]	0.293	0.268	0.239	0.325	0.292	0.291	0.285	0.029	10.092
$\rho_{g,\omega}$	[kg/m^3]	453	424	483	459	433	463	452	21.3	4.7
$\rho_{g,0,\omega}$	[kg/m^3]	402	378	431	408	385	411	402	19.0	4.7
ω_g	[%]	12.6	12.3	12.1	12.5	12.3	12.6	12.4	0.2	1.7
$\rho_{c,\omega}$	[kg/m^3]	449	468	483	470	430	440	457	20.4	4.5
$\rho_{c,0,\omega}$	[kg/m^3]	398	417	430	415	381	389	405	18.8	4.6
ω_c	[%]	12.8	12.4	12.4	13.2	12.8	13.2	12.8	0.4	2.9

Table B-8: Detailed test results - Test series S8_1NP-200

Test Series	S8_1NP-200								
Test specimen		**1**	**2**	**3**	**4**	**5**	**6**	**Mean**	**St.dev**	**CoV (%)**
F_{est}	[kN]	35	35	35	35	35	35			
F_{04}	[kN]	14	14	14	14	14	14			
F_{01}	[kN]	3.5	3.5	3.5	3.5	3.5	3.5			
A	[mm^2]	14400	14400	14400	14400	14400	14400			
t_i	[mm]	1.3	1.3	1.3	1.3	1.3	1.3			
v_{01}	[mm]	0.035	0.031	0.031	0.034	0.033	0.029	0.032	0.002	6.703
v_{04}	[mm]	0.226	0.236	0.241	0.210	0.248	0.213	0.229	0.015	6.651
v_{14}	[mm]	0.246	0.262	0.272	0.231	0.273	0.235	0.253	0.019	7.356
v_{11}	[mm]	0.151	0.158	0.168	0.133	0.171	0.148	0.155	0.014	8.881
v_{21}	[mm]	0.142	0.145	0.168	0.131	0.174	0.147	0.151	0.016	10.757
v_{24}	[mm]	0.252	0.266	0.278	0.235	0.281	0.239	0.258	0.020	7.604
$v_{0,6}$	[mm]	0.528	0.512	0.631	0.522	0.547	0.616	0.559	0.051	9.163
$v_{0,8}$	[mm]	1.576	1.431	1.682	1.635	1.523	1.477	1.554	0.095	6.125
v_{max}	[mm]	5.954	5.478	5.084	5.424	4.620	4.987	5.258	0.463	8.804
v_f	[mm]	9.101	9.908	8.226	7.484	7.607	8.508	8.472	0.921	10.875
F_{max}	[kN]	33.021	31.935	32.716	33.661	31.727	34.500	32.927	1.048	3.183
F_{max}/A	[N/mm^2]	2.293	2.218	2.272	2.338	2.203	2.396	2.287	0.073	3.183
$v_{i,mod}$	[mm]	0.254	0.272	0.280	0.236	0.287	0.246	0.263	0.020	7.730
v_s	[mm]	-0.028	-0.037	-0.039	-0.025	-0.039	-0.032	-0.033	0.006	-16.887
v_e	[mm]	0.137	0.150	0.143	0.134	0.140	0.118	0.137	0.011	7.781
k_i	[kN/mm]	61.942	59.409	57.979	66.545	56.452	65.625	61.325	4.117	6.713
k_s	[kN/mm]	55.033	51.423	49.957	59.403	48.837	56.962	53.602	4.189	7.814
$v_{i,mod}$-v_{24}	[mm]	0.002	0.006	0.003	0.001	0.006	0.007	0.004	0.003	62.274
Specific slip values and ductility evaluation										
$u_{y,EN}$	[mm]	0.274	0.267	0.267	0.263	0.267	0.264	0.267	0.004	1.479
$u_{max} = v_{max}$	[mm]	5.954	5.478	5.084	5.424	4.620	4.987	5.258	0.463	8.804
$u_f = v_f$	[mm]	9.101	9.908	8.226	7.484	7.607	8.508	8.472	0.921	10.875
$D_f = u_f / u_{y,EN}$	[-]	33.193	37.126	30.864	28.465	28.441	32.239	31.721	3.279	10.335
$D_u = u_{max} / u_{y,EN}$	[-]	21.716	20.525	19.074	20.629	17.274	18.896	19.686	1.583	8.042
$D_{uy} = u_{max} - u_{y,EN}$	[mm]	5.680	5.211	4.817	5.161	4.353	4.723	4.991	0.461	9.232
$D_{fy} = u_f - u_{y,EN}$	[mm]	8.826	9.641	7.959	7.221	7.339	8.244	8.205	0.920	11.208
$D_{fu} = u_f - u_{max}$	[mm]	3.147	4.430	3.142	2.060	2.987	3.521	3.215	0.770	23.962
$u_{y,05Fmax}$	[mm]	0.321	0.313	0.355	0.309	0.328	0.352	0.330	0.020	5.934
$u_{y,04\text{-}09}$	[mm]	0.312	0.294	0.295	0.299	0.292	0.281	0.296	0.010	3.471
$u_{y,CSIRO}$	[mm]	0.252	0.243	0.259	0.245	0.250	0.256	0.251	0.006	2.432
$\rho_{g,\omega}$	[kg/m^3]	460	419	449	502	494	512	473	35.7	7.6
$\rho_{g,0,\omega}$	[kg/m^3]	406	372	398	444	438	452	418	31.3	7.5
ω_g	[%]	13.2	12.7	13.0	13.0	12.8	13.1	13.0	0.2	1.5
$\rho_{c,\omega}$	[kg/m^3]	418	482	463	437	408	466	446	29.2	6.5
$\rho_{c,0,\omega}$	[kg/m^3]	368	423	409	385	358	409	392	25.8	6.6
ω_c	[%]	13.5	13.9	13.2	13.6	14.1	14.0	13.7	0.4	2.6

Table B-9: Detailed test results - Test series SA_1NP-200

Test Series	SA_1NP-200							
Test specimen		**2**	**3**	**4**	**5**	**6**	**Mean**	**St.dev**	**CoV (%)**
F_{est}	[kN]	30	30	30	30	30			
F_{04}	[kN]	12	12	12	12	12			
F_{01}	[kN]	3	3	3	3	3			
A	[mm^2]	14400	14400	14400	14400	14400			
t_i	[mm]	1.3	1.3	1.3	1.3	1.3			
v_{01}	[mm]	0.031	0.037	0.029	0.033	0.033	0.032	0.003	9.137
v_{04}	[mm]	0.215	0.214	0.198	0.188	0.226	0.208	0.015	7.186
v_{14}	[mm]	0.228	0.230	0.200	0.201	0.243	0.220	0.019	8.689
v_{11}	[mm]	0.110	0.115	0.104	0.094	0.132	0.111	0.014	12.900
v_{21}	[mm]	0.108	0.114	0.103	0.093	0.129	0.109	0.013	12.237
v_{24}	[mm]	0.231	0.234	0.207	0.200	0.246	0.223	0.019	8.622
$v_{0,6}$	[mm]	0.608	0.619	0.809	0.543	0.605	0.637	0.101	15.833
$v_{0,8}$	[mm]	1.537	1.776	1.818	1.486	1.421	1.608	0.179	11.113
v_{max}	[mm]	4.545	5.418	6.146	4.649	5.587	5.269	0.671	12.737
v_f	[mm]	7.506	6.199	6.508	4.904	7.815	6.586	1.155	17.543
F_{max}	[kN]	32.922	32.492	36.568	32.998	30.857	33.167	2.088	6.297
F_{max}/A	[N/mm^2]	2.286	2.256	2.539	2.292	2.143	2.303	0.145	6.297
$v_{i,mod}$	[mm]	0.245	0.237	0.226	0.207	0.257	0.234	0.019	8.247
v_s	[mm]	-0.030	-0.023	-0.028	-0.018	-0.032	-0.026	0.006	-21.171
v_e	[mm]	0.160	0.156	0.134	0.143	0.152	0.149	0.011	7.186
k_i	[kN/mm]	55.800	56.023	60.695	63.741	53.179	57.887	4.247	7.337
k_s	[kN/mm]	48.961	50.692	53.201	58.087	46.651	51.518	4.385	8.511
$v_{i,mod}$-v_{24}	[mm]	0.015	0.003	0.018	0.007	0.011	0.011	0.006	56.543
Specific slip values and ductility evaluation									
$u_{y,EN}$	[mm]	0.377	0.361	0.384	0.319	0.388	0.366	0.028	7.697
$u_{max} = v_{max}$	[mm]	4.545	5.418	6.146	4.649	5.587	5.269	0.671	12.737
$u_f = v_f$	[mm]	7.506	6.199	6.508	4.904	7.815	6.586	1.155	17.543
$D_f = u_f / u_{y,EN}$	[-]	19.903	17.194	16.967	15.372	20.121	17.912	2.043	11.408
$D_u = u_{max} / u_{y,EN}$	[-]	12.052	15.028	16.023	14.571	14.384	14.412	1.464	10.156
$D_{uy} = u_{max} - u_{y,EN}$	[mm]	4.168	5.057	5.762	4.329	5.198	4.903	0.656	13.370
$D_{fy} = u_f - u_{y,EN}$	[mm]	7.128	5.838	6.124	4.585	7.426	6.220	1.130	18.166
$D_{fu} = u_f - u_{max}$	[mm]	2.961	0.781	0.362	0.256	2.228	1.317	1.210	91.853
$u_{y,05Fmax}$	[mm]	0.391	0.389	0.491	0.347	0.383	0.400	0.054	13.494
$u_{y,04\text{-}09}$	[mm]	0.377	0.383	0.384	0.333	0.370	0.369	0.021	5.670
$u_{y,CSIRO}$	[mm]	0.318	0.317	0.353	0.280	0.317	0.317	0.026	8.083
$\rho_{g,\omega}$	[kg/m^3]	429	473	435	450	469	451	19.7	4.4
$\rho_{g,0,\omega}$	[kg/m^3]	382	419	387	397	416	400	16.7	4.2
ω_g	[%]	12.2	13.0	12.3	13.3	12.7	12.7	0.5	3.7
$\rho_{c,\omega}$	[kg/m^3]	395	387	442	373	435	406	30.4	7.5
$\rho_{c,0,\omega}$	[kg/m^3]	354	345	395	334	389	363	27.1	7.5
ω_c	[%]	11.6	12.2	11.9	11.7	11.8	11.8	0.2	1.9

Appendix C. Yield slip evaluation on single load-slip curves

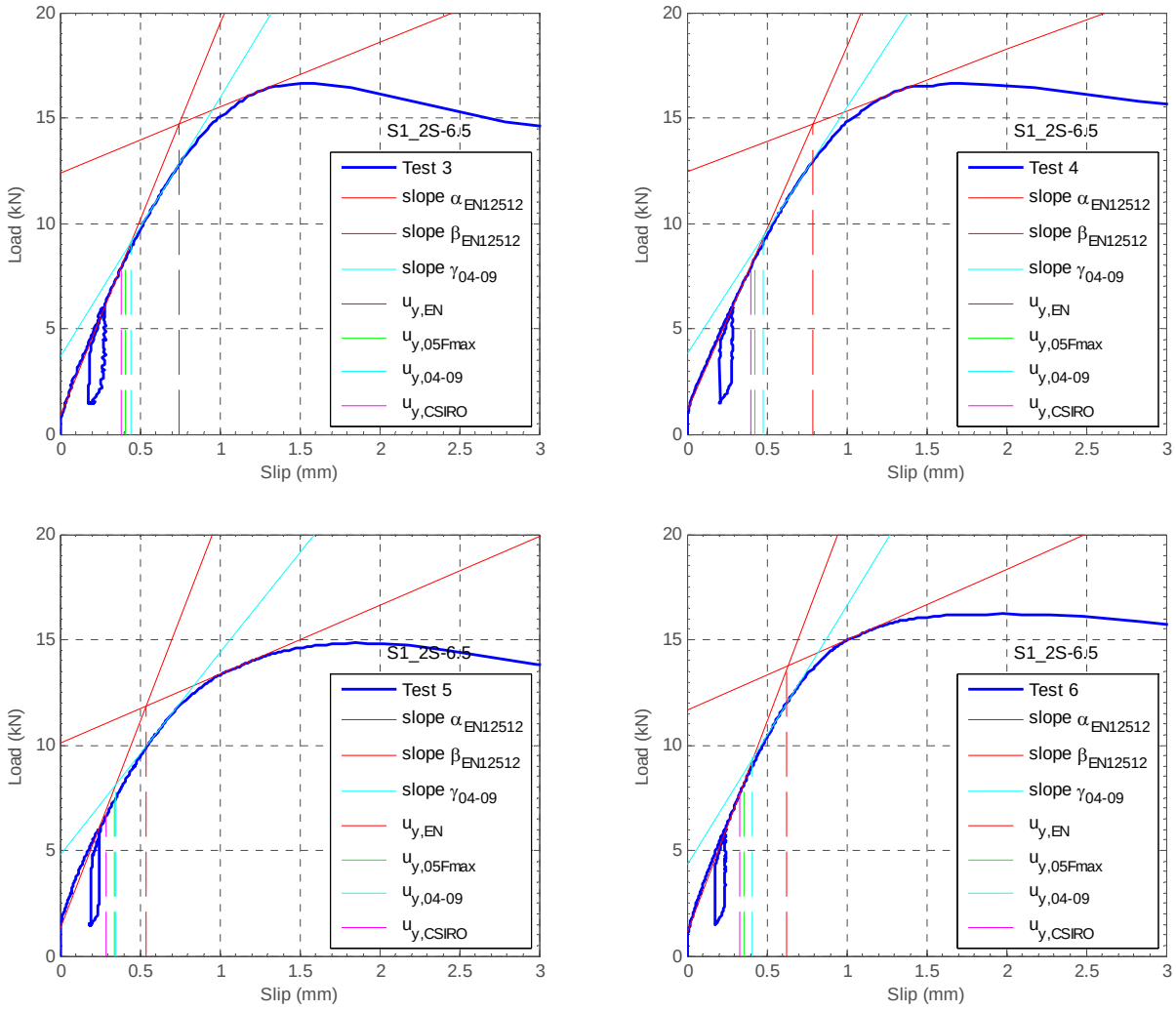

Fig. C-1: Test series S1_2S-6.5

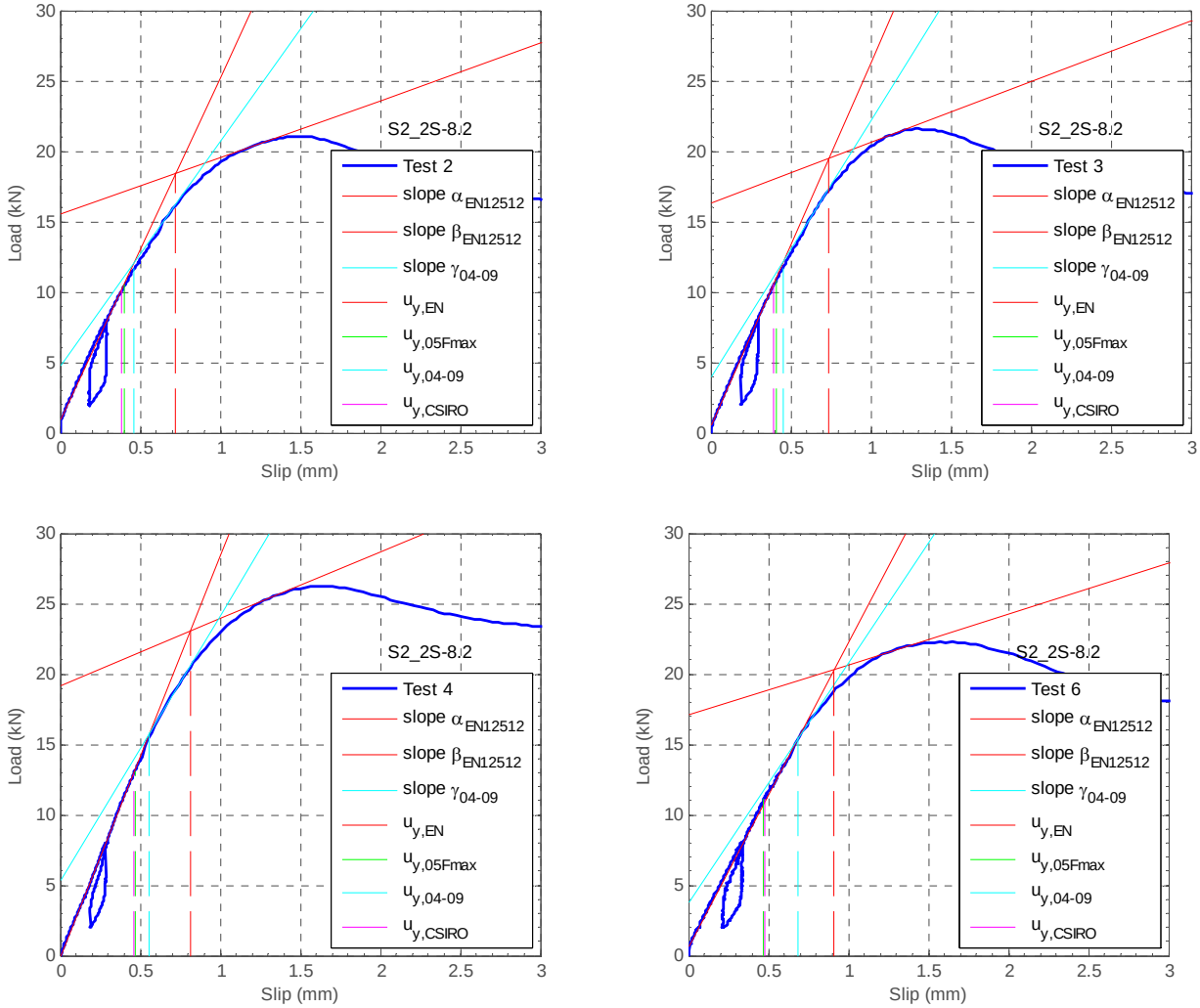

Fig. C-2: Test series S2_2S-8.2

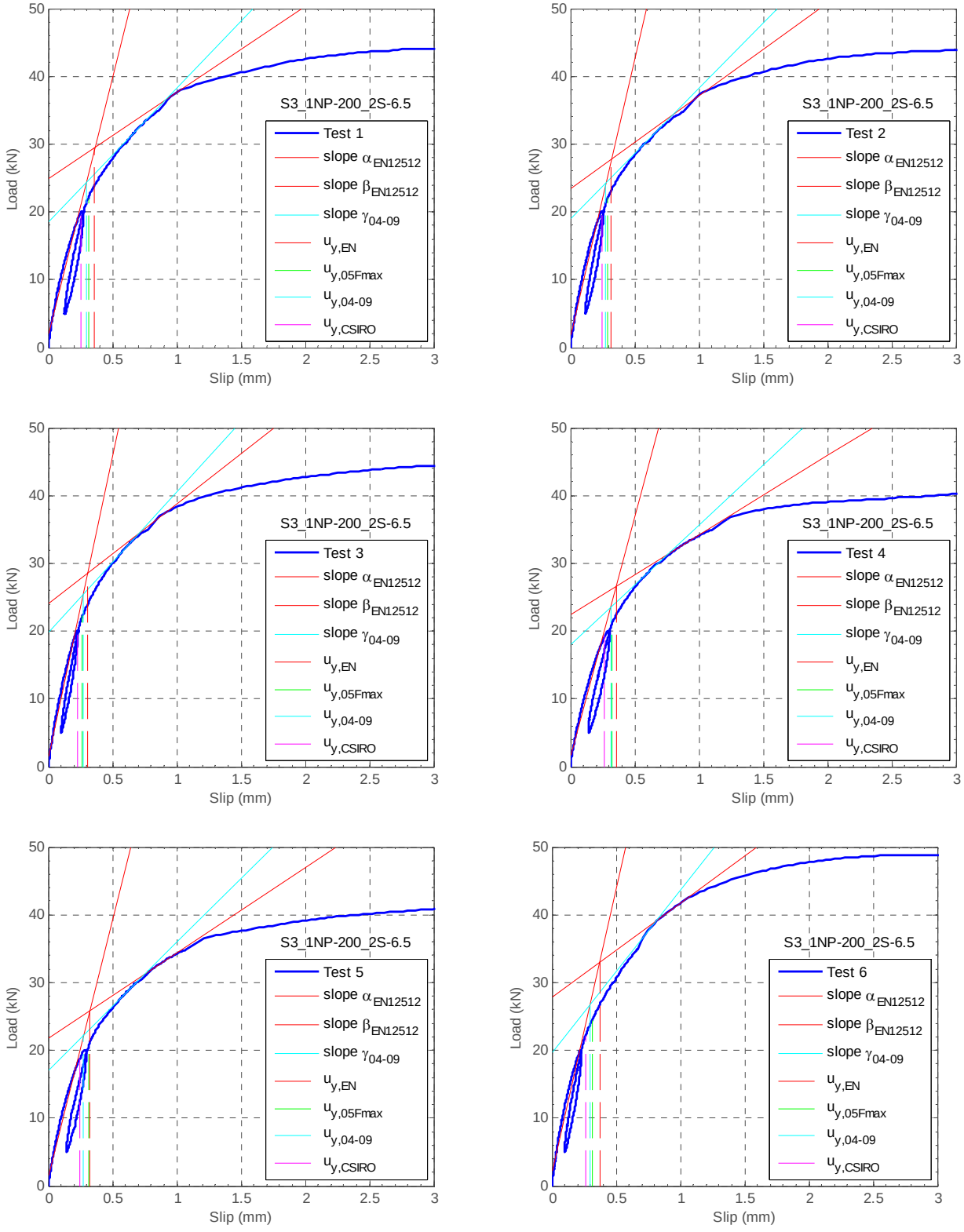

Fig. C-3: Test series S3_1NP-200/2S-6.5

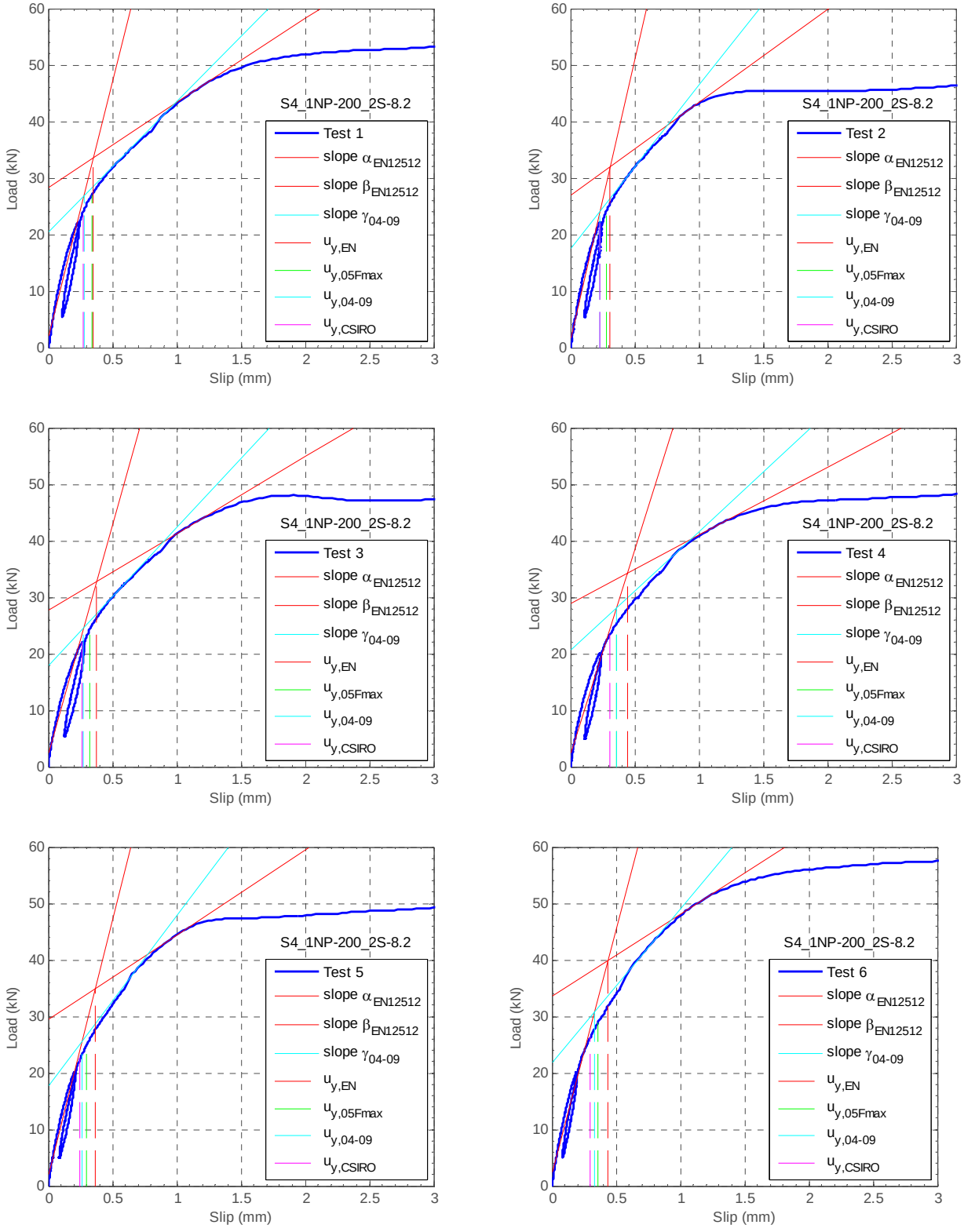

Fig. C-4: Test series S4_1NP-200/2S-8.2

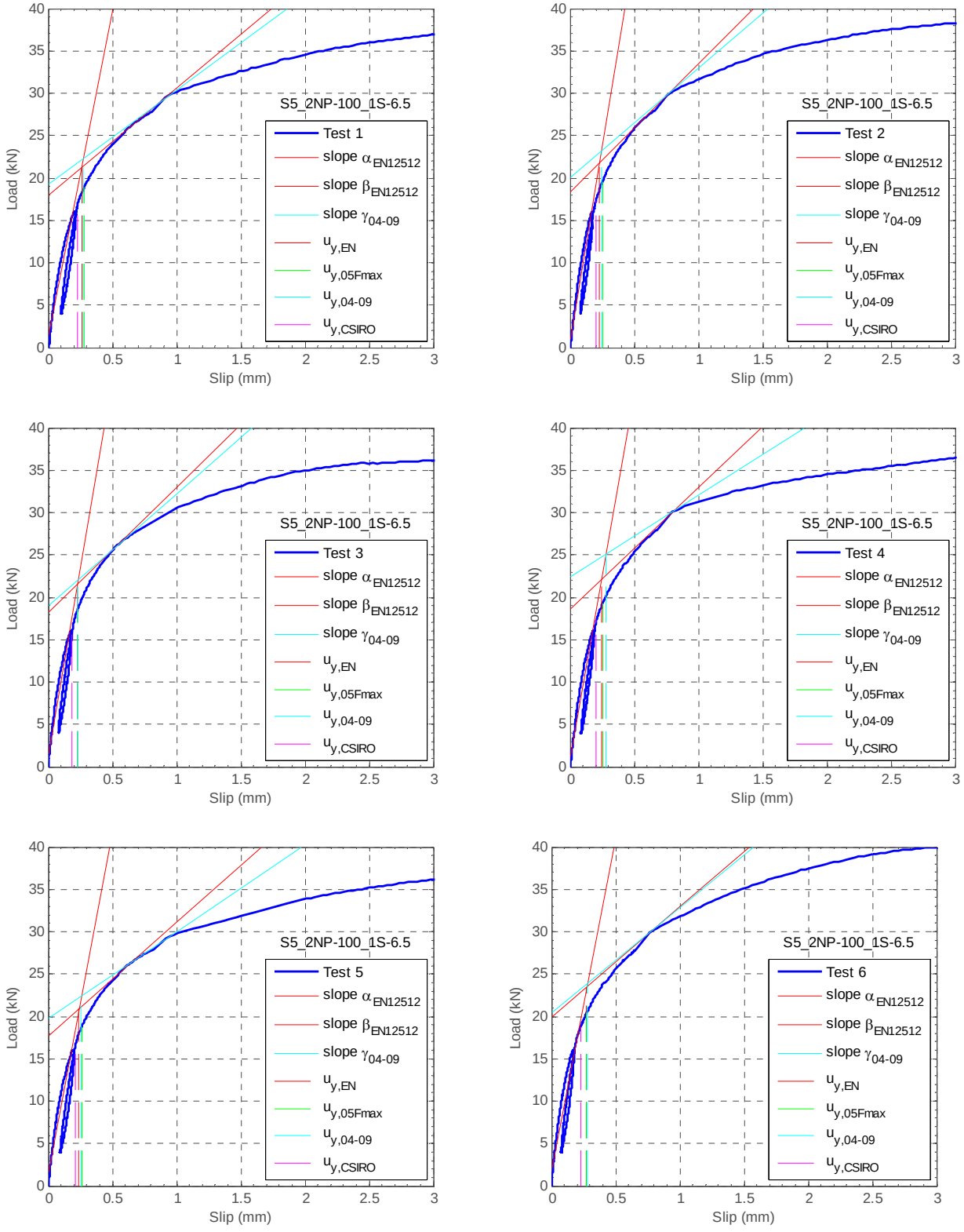

Fig. C-5: Test series S5_2NP-100/1S-6.5

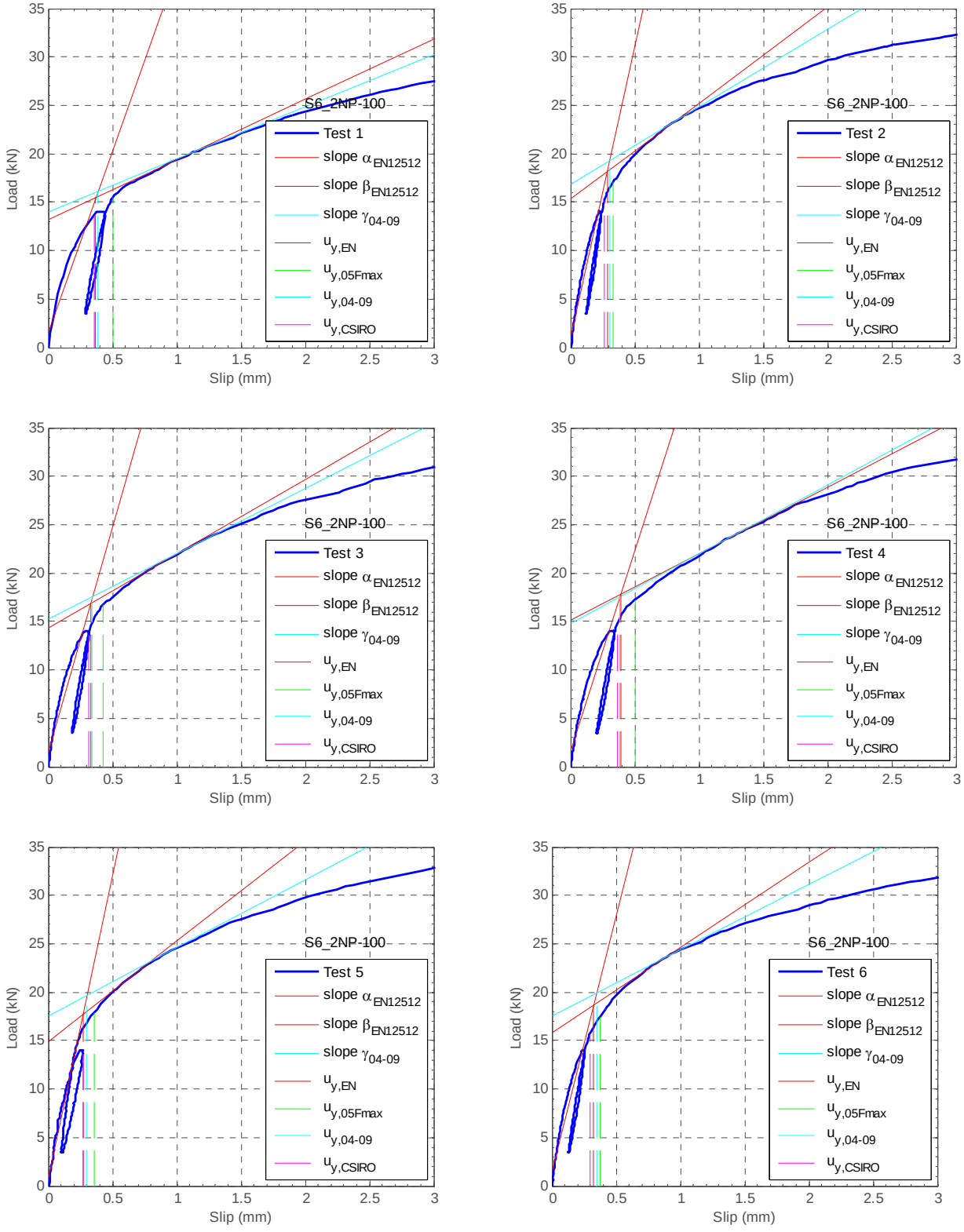

Fig. C-6: Test series S6_2NP-100

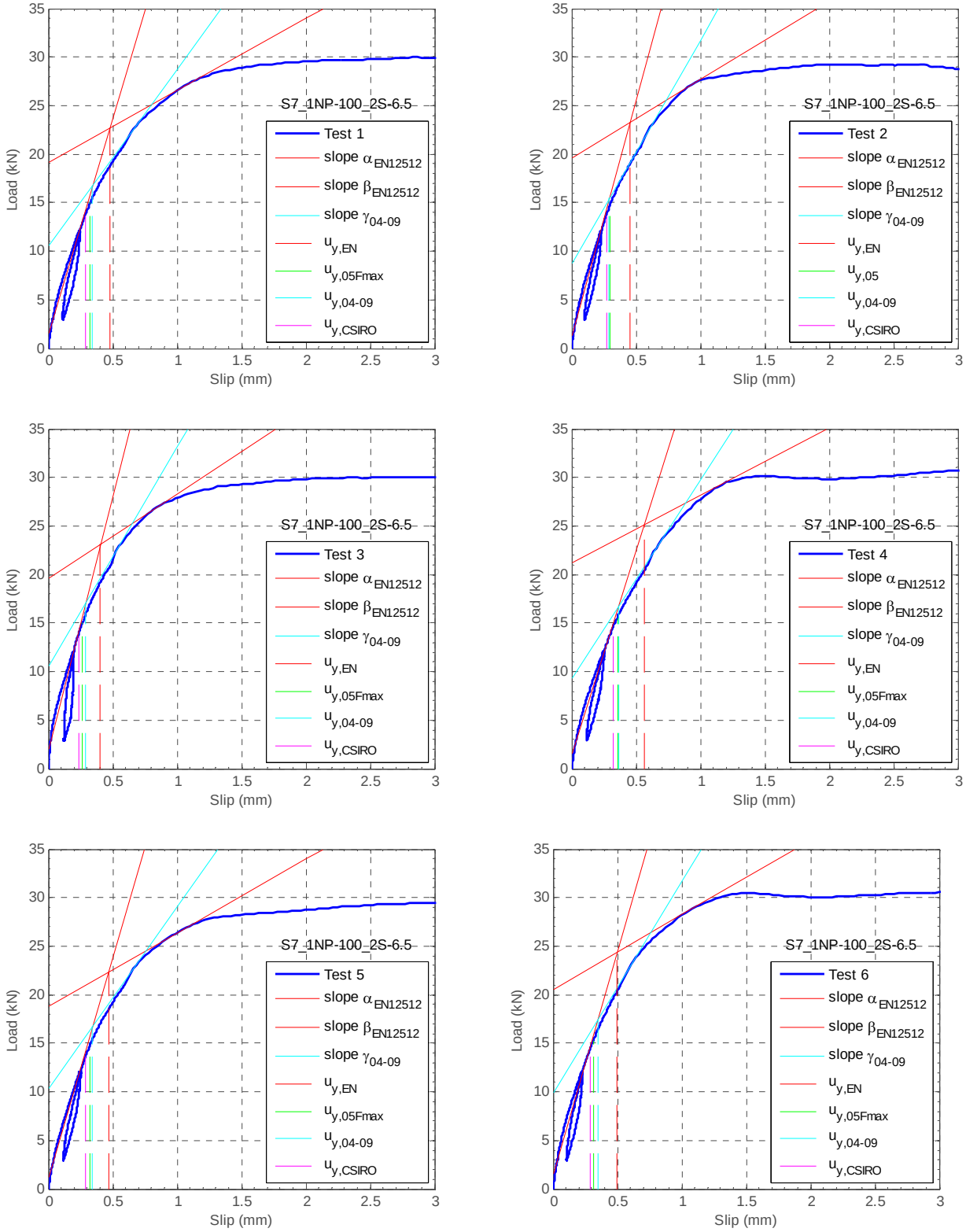

Fig. C-7: Test series S7_1NP-100/2S-6.5

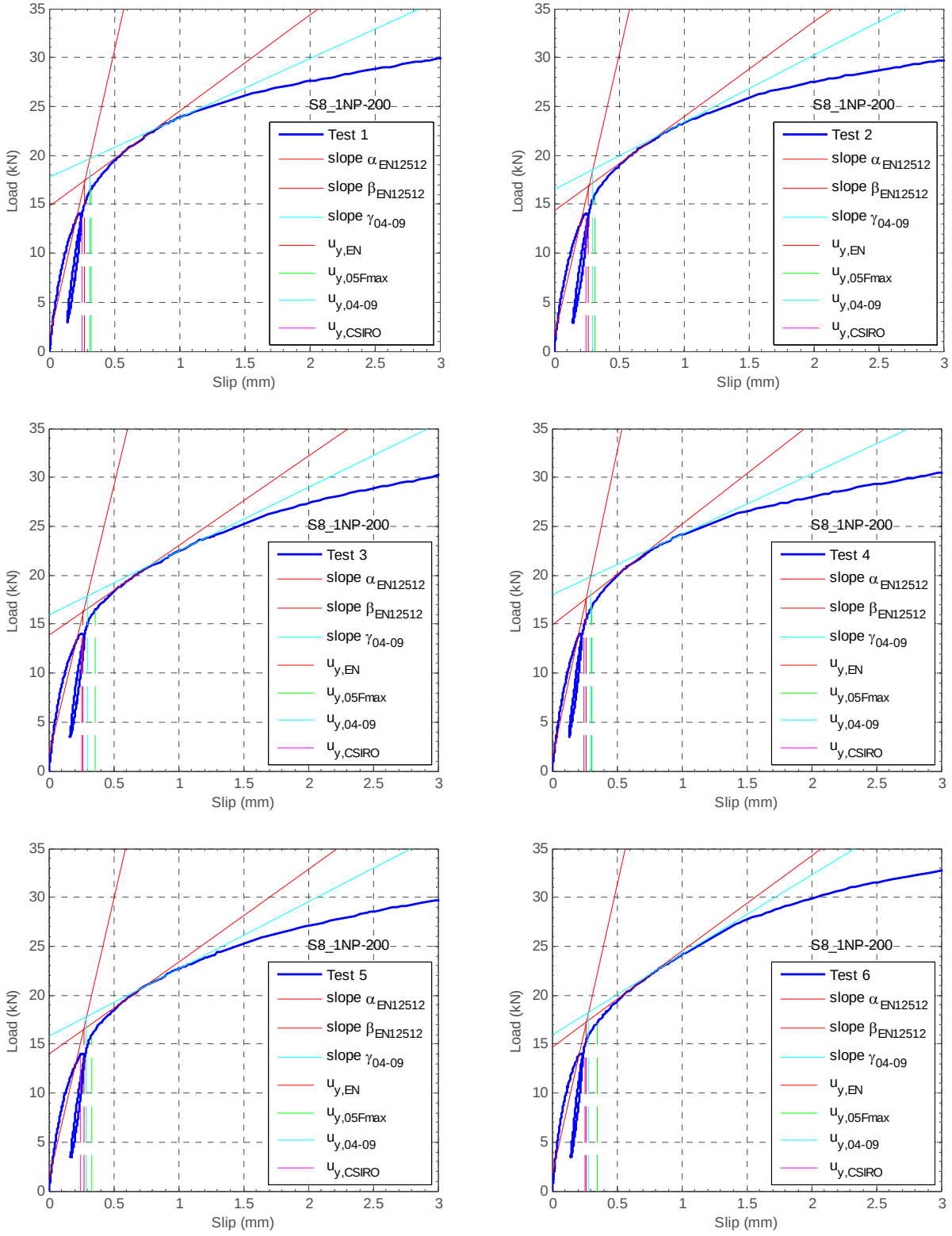

Fig. C-8: Test series S8_1NP-200

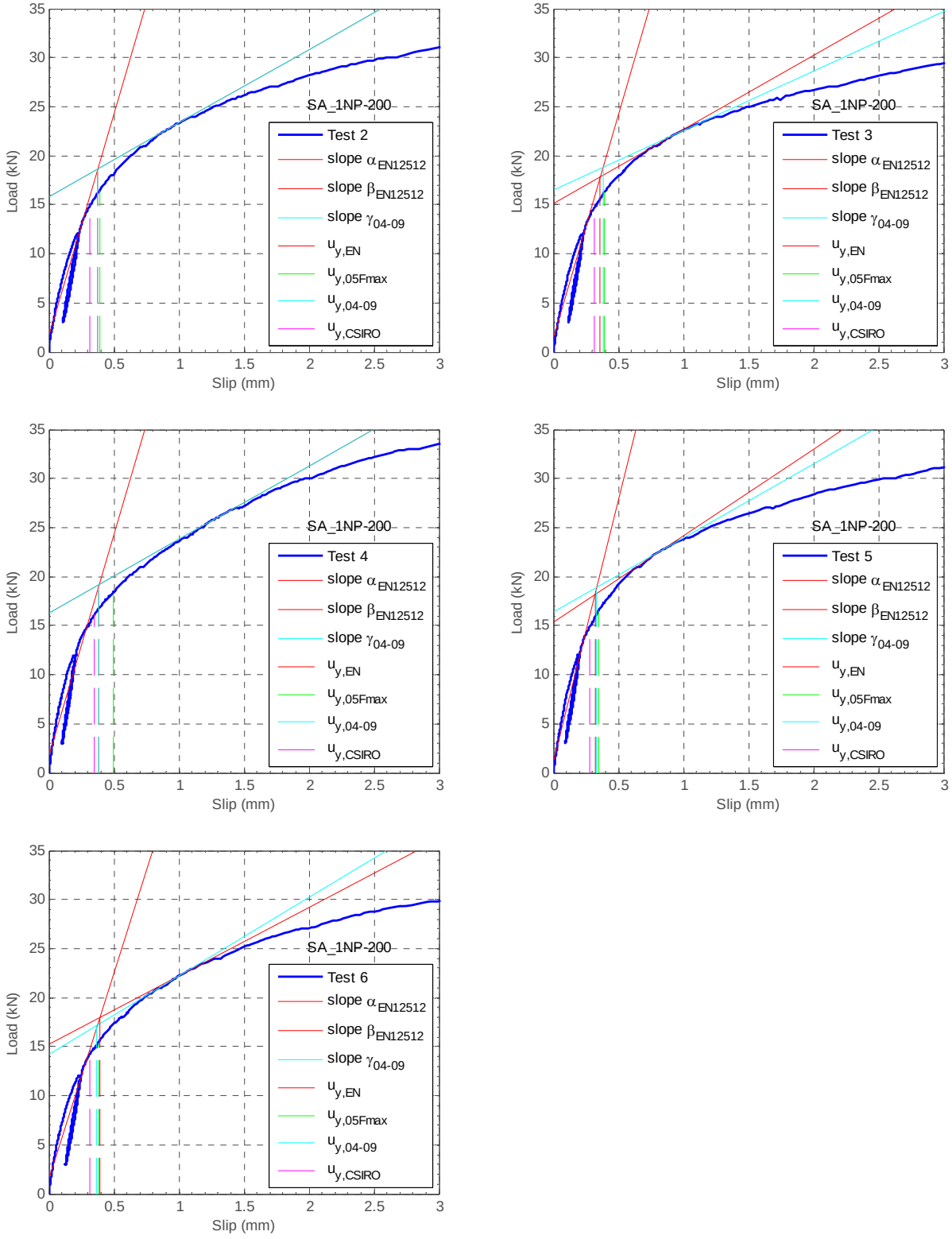

Fig. C-9: Test series SA_1NP-200

Appendix D. Withdrawal tests on double-sided nail plate joint with and without screws

In addition to the shear tests, simple withdrawal tests were performed in order to obtain an estimate of the actual withdrawal capacity of the double-sided nail plate. Fig. D-1 shows pictures of the installation of the double-sided nail plate and of the withdrawal test setup.

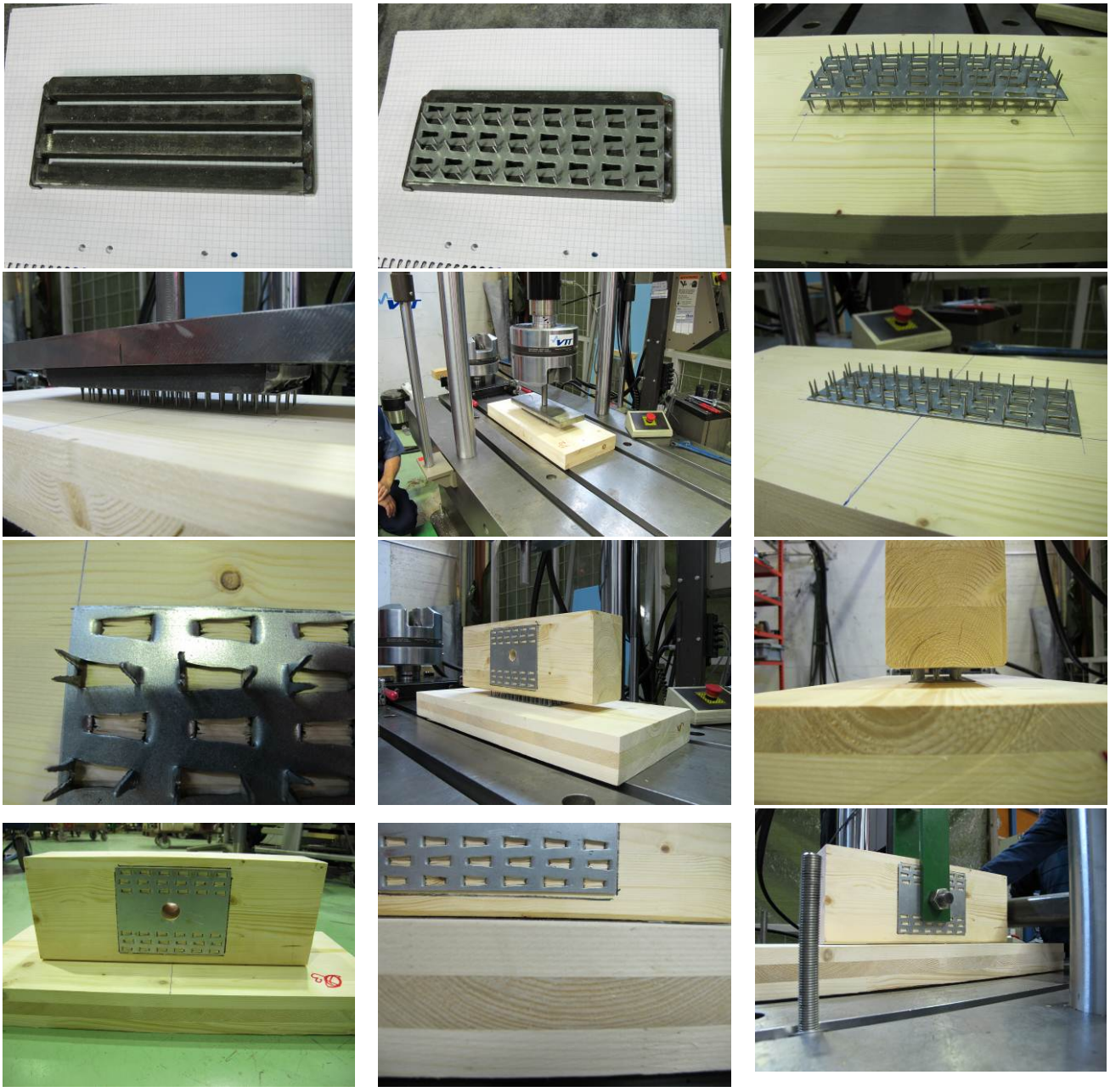

Fig. D-1: Pictures of the fabrication and of the test setup for the withdrawal tests with double-sided nail plates

Two tests were performed:

- One withdrawal test with one Sepa-SE2P double-sided nail plate only (72×200 mm)
- One withdrawal test with one Sepa-SE2P double-sided nail plate (72×200 mm) and two vertical WT-T screws (6.5×160 mm) passing through the nail plate

One aim of this test was to verify if the screws could be installed through the double-sided nail plate without predrilling. The other aim was to obtain an estimate of the capacity of the double-sided nail plate only, compared with the capacity of screw against separation forces.

The installation of the screws through the nail plate could be done without problem. The screw went through the flat plain part of the nail plate and only a slight resistance was felt when drilling through the nail plate. We should note however that a good level of precision is necessary in order to make sure that the screws do not pass through one of the holes of the nail plate.

The load-displacement curves for both tests are presented in Fig. D-2.

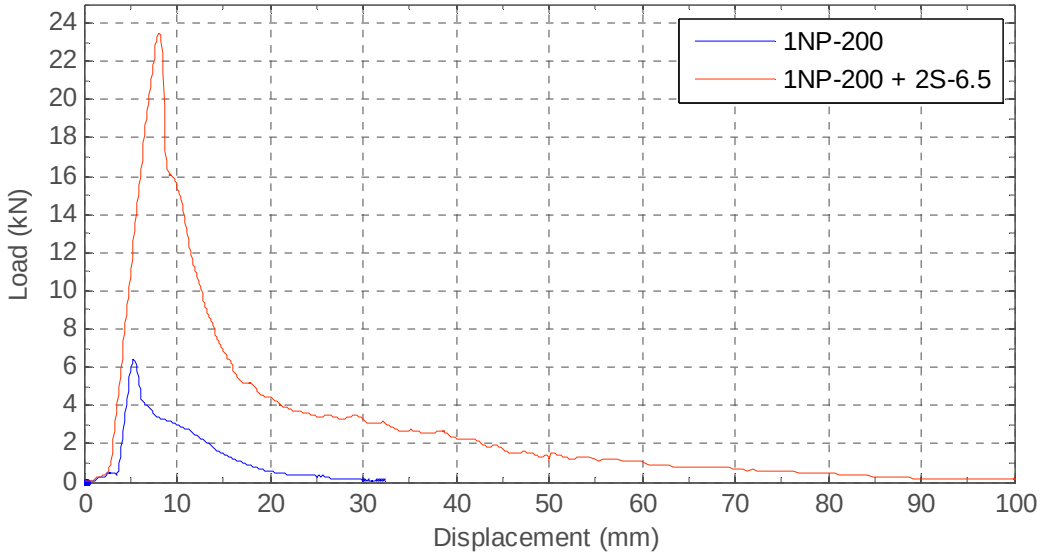

Fig. D-2: Load displacement curves from withdrawal tests for SE2P nail plates (length 200mm) only, and for SE2P nail plates (length 200mm) with two 6.5 mm WT-screws

Table D-1: Withdrawal test results

Test name	Maximum load	Displacement at maximum load
	kN	mm
1NP-200	6.43	5.332
1NP-200 + 2S-6.5	23.50	8.12

Assuming that the 72×200 mm double-sided nail plate contributes with the same ultimate capacity of 6.43 kN in the test configuration with two screws, the contribution from one screw can be estimated to be about 8.54 kN. In that respect, the double-sided nail plate exhibited a relatively high load-carrying capacity for connectors that theoretically have no withdrawal capacity. However, these results should be considered with care. Only one test was performed for each configuration and the results obtained reflect the capacity of the double-sided nail plate loaded under pure separation forces. Combined with shear forces, the behaviour might

be different. Pictures of the tests specimens during testing and after failure are presented in Fig. D-3 and Fig. D-4 for the tests without and with screws, respectively.

Table 7: Pictures of the withdrawal tests with Sepa-SE2P double-sided nail plates only

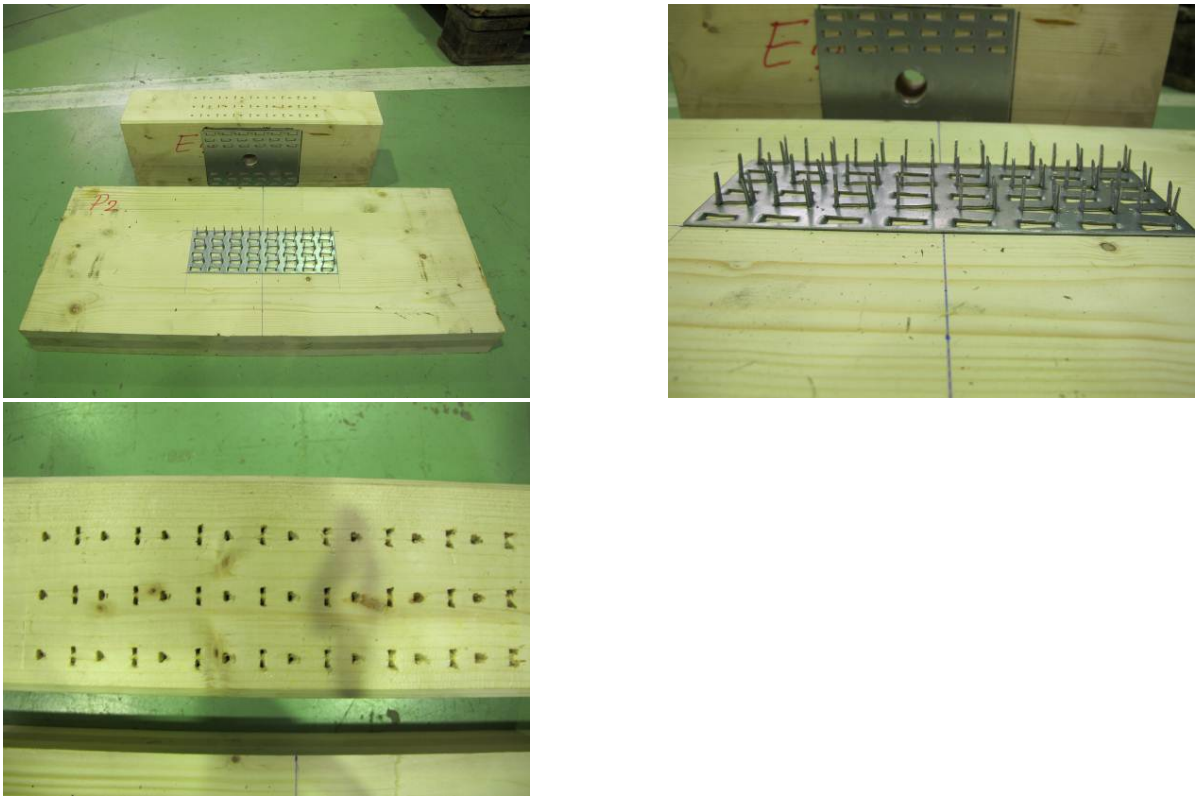

Fig. D-3: Pictures of the withdrawal tests with Sepa-SE2P double-sided nail plates only

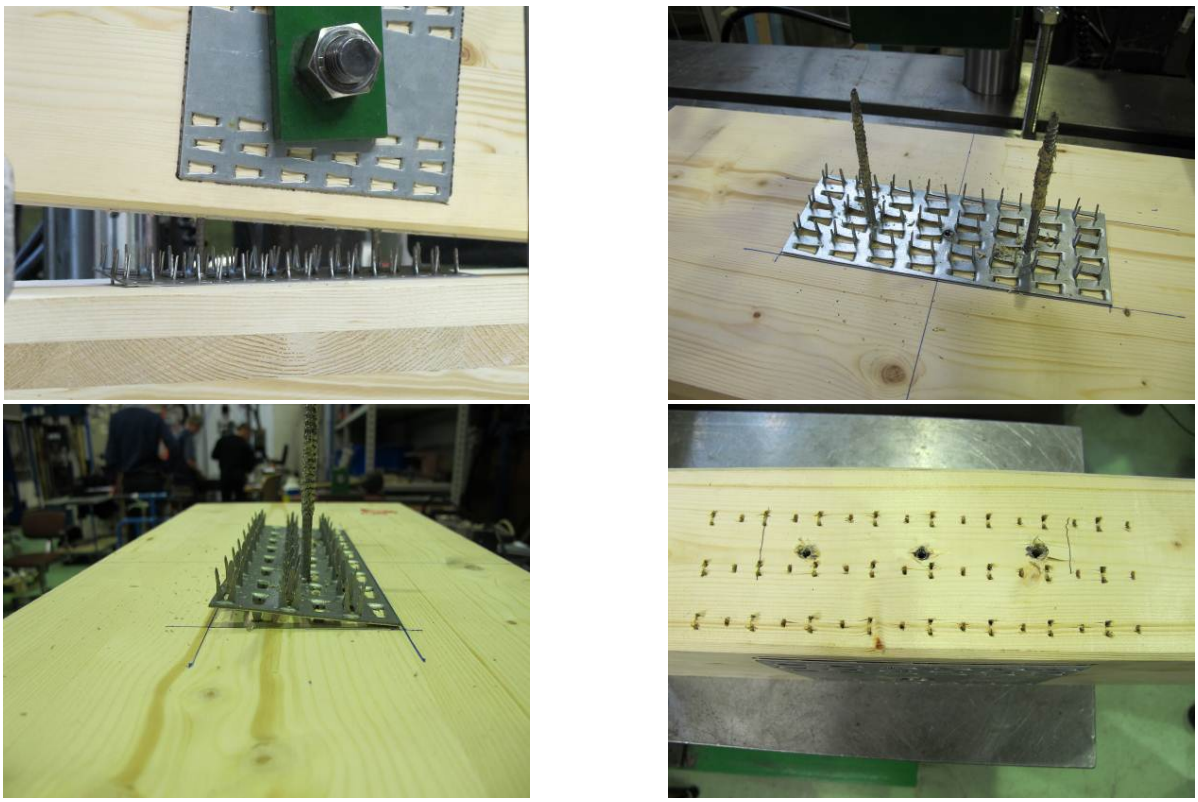

Fig. D-4: Pictures of the withdrawal tests with Sepa-SE2P double-sided nail plates and two SFS WT screws

After the withdrawal test, it was possible to observe that the threads of the screws were damaged after passing through the steel plate since the WT-screws are designed to drill through timber. This might affect the withdrawal capacity of the screws. It should also be noted that the screws (160 mm long) were not exactly appropriate for drilling at 90 degrees and shorter screws would need to be used instead for that purpose (90 mm or 130 mm long WT-screws for example). These have both a threaded part 40 mm long. Comparing with the 65 mm long thread of the 160 mm long screws, they should have a lower withdrawal capacity. They might as well provide less force to drill through the steel plate for that reason also.

References

[1] European Committe for Standardization (CEN), "EN 1075:1999 - Timber Structures - Test methods – Joints made with punched metal plate fasteners," ed. Brussels, 1999.

[2] European Committe for Standardization (CEN), "EN 26891:1991 - Timber structures - Joints made with mechanical fasteners - General principles for the determination of strength and deformation characteristics," ed, 1991.

[3] A. Kevarinmäki, "Lausunto nro VTT-S-02797-12 - Naulalevylausunto kaksipuoleiselle SE2P naulalevylle," VTT Expert Services Oy VTT-S-02797-12, 2012.

[4] Ö. I. f. B. (OIB). (2012) European technical approval ETA-12/0063 - SFS self-tapping screws WT. 18. Available: http://www.sfsintec.biz/internet/sfsmedien.nsf/EF334F61A18A1D69C1257B020056520F/$FILE/66115_ETA_en_WT_ELECTRONIC.pdf

[5] European Committe for Standardization (CEN), "SS-EN 1194:1999 - Glued laminated timber - Strength classes and determination of characteristic values," vol. SS-EN 1194:1999 Sv, ed: Swedish Institute for Standards (SIS), 1999.

[6] D. I. f. B. (DIBt), "European Technical Approval ETA-08/0271 - CLT - Cross Laminated Timber," in ETA-08/0271, European Organisation for Technical Approvals (EOTA), Ed., ed, 2011, p. 17.

[7] European Committe for Standardization (CEN), "EN 28970:1991 - Timber structures - Testing of joints made with mechanical fasteners - Requirements of wood density ", ed, 1991.

[8] A. Kevarinmäki, "Research Report - No VTT-S-02784-12 -Testing of double sided SE2P nail plate for glulam-CLT shear connector," VTT Expert Services Oy, Finland, 2012.

[9] A. Kevarinmäki, "Research Report - No VTT-S-01096-13 -Testing of double sided SE2P nail plates with SFS-WT screws for glulam-CLT shear connection," VTT Expert Services Oy, Finland, 2013.

[10] A. Jorissen and M. Fragiacomo, "General notes on ductility in timber structures," Engineering Structures, vol. 33, pp. 2987-2997, 2011.

[11] W. Muñoz, M. Mohammad, A. Salenikovich, and P. Quenneville, "Need for a harmonized approach for calculations of ductility of timber assemblies," presented at the CIB W18, St. Andrews, Canada, 2008.

[12] European Committe for Standardization (CEN), "EN 12512:20014 - Timber strucutres - Test methods - Cyclic testing of joints made with mechanical fasteners," ed. Brussels, 2001.

[13] L. Stehn and A. Björnfot, "Comparison of different ductility measures for a nailed steel-to-timber connection," presented at the 7th World conference on timber engineering : WCTE 2002, Shah Alam, Malaysia, 2002.

[14] S. Gagnon and C. Pirvu, CLT Handbook Cross-Laminated Timber - Canadian Edition. Québec: FP Innovations, 2011.

[15] R. Tomasi, A. Crosatti, and M. Piazza, "Theoretical and experimental analysis of timber-to-timber joints connected with inclined screws," Construction and Building Materials, vol. 24, pp. 1560-1571, 2010.